CHEMISTRY
A European Journal

Supporting Information

Efficient Detection of Structure and Dynamics in Unlabeled RNAs: The SELOPE Approach

Judith Schlagnitweit, Emilie Steiner, Hampus Karlsson, and Katja Petzold*[a]

chem_201800992_sm_miscellaneous_information.pdf

1. ^{1}H-^{1}H 2D SELOPE

1.1 Sample preparation

Both, the GUG, as well as the GUC construct, investigated in this work were prepared by in vitro transcription using T7 RNA polymerase (produced in house by PSF), unlabeled nucleotide triphosphates (Sigma) and synthetic DNA templates (IDT) containing the T7 promoter and sequence of interest. The RNA was purified by HPLC and exchanged into NMR buffer (15 mM sodium phosphate, 0.1 mM EDTA and 25 mM NaCl at pH 6.5) multiple times. Final sample concentrations for GUG and GUC are ~2mM.

1.2 Experimental details

Experiments were carried out on a Bruker Avance III spectrometer operating at 600 MHz (^{1}H resonance frequency) and equipped with a 5mm QCI (^{1}H/^{13}C/^{15}N/^{31}P) cryoprobe. NMR spectra were acquired and processed using Bruker Topspin 3.2 software.

The 2D pulse sequence is presented in Figure 2a of the main text. Filled and open rectangles correspond to 90º and 180º hard pulses, respectively. Filled semioval shapes indicate 90º shaped pulses for selective excitation of the H8/H6 or H5/H1' region of the proton spectrum. 4 or 5.5 ms Eburb2 shaped pulses[1] were used, respectively. The coherence transfer delay τ was set to 1 / (4 $^{3}J_{HH}$) corresponding to a 25-30 ms delay. In this work we used an excitation sculpting scheme[2] for water suppression. It has to be noted that this can easily be replaced by other water suppression methods such as Watergate[3]. The carrier frequency is set to the peak or the centre of the region of interest (H8/H6 or H5/H1'), except during the water suppression block where it is moved to the water resonance. The displayed gradients are purge gradients. States-TPPI[4] was used for quadrature detection in the indirect dimension.

1.3 2D SELOPE spectra for GUG

1.3.1 H8/H6-H5 2D and HSQC for comparison

Figure S01 shows the diagonal of the H8/H6-H5 2D spectrum as overlay with a ^{1}H-^{13}C HSQC. The H8 diagonal and the H6-H5 cross peak region are shown in the main article in Figure 2. For these spectra 44 FIDs were recorded for an indirect dimension of 1.8 ppm spectral width. 16 scans were recorded per increment with a recovery delay of 1.5 s leading to an overall experimental time of 27 min.

Figure S01

^{1}H-^{13}C HSQC of the GUG RNA construct including assignment. 128 scans were recorded per increment (number of increments = 256 for sw = 30 ppm) with a recovery delay of 1.5 s leading to an overall experimental time of 15 h 17 min.
The spectrum is overlaid with the projection of the H8 diagonal of the H8 / H6-H5 2D spectrum to show the depletion effect.

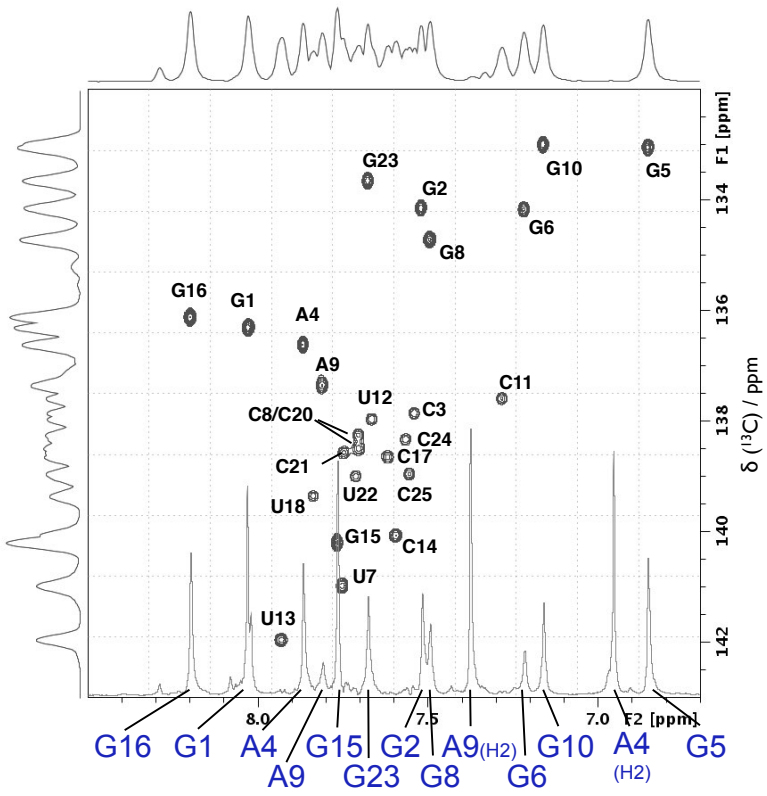

1.3.2 H1'-H2'/H5-H6 2D

Starting with selective excitation of the H5/H1' region it is possible to obtain a 2D spectrum with H5-H6 cross peaks and H1' peaks along the diagonal as shown in Figure S02.

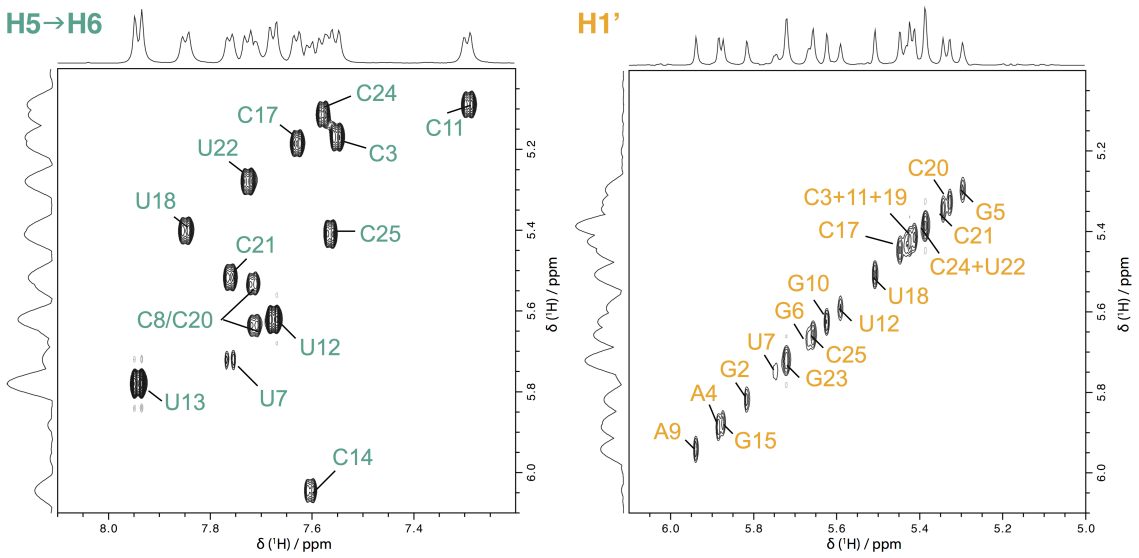

Figure S02. H1'/H5-H6 spectrum of the GUG construct. 30 FIDs were recorded for an indirect dimension of 1.2 ppm spectral width. 32 scans were co-added with a recovery delay of 1.5 s leading to an overall experimental time of 37 min.

For H1' it depends on the sugar pucker conformation whether the magnetization stays on H1', i.e. along the diagonal in the spectrum (in the case of the sugar pucker being in C3'-endo conformation where ^{3}J coupling constants between H1' and H2' are < 2 Hz [5,6]), or is transferred to H2' leading to H1'-H2' cross peaks for residues with different sugar conformations with larger ^{3}J(H1'-H2') coupling constants such as the C2'-endo form (~8 Hz[5,6], similar to ^{3}J(H5-H6)). Figure S03 shows the H1'-H2' region of the 2D spectrum shown above.

Figure S03

H1'-H2' region of the acquired 2D spectrum of Figure S02. Using the τ delay optimized for fully transferring H5 coherence to H6, magnetization is also transferred for residues which are not in the for RNA usual C3'-endo conformation. In the sample studied here, magnetization is fully transferred from H1' to H2' for C14 and partially for U7 and G6 indicating a mixed C2'/C3' endo state for those protons.

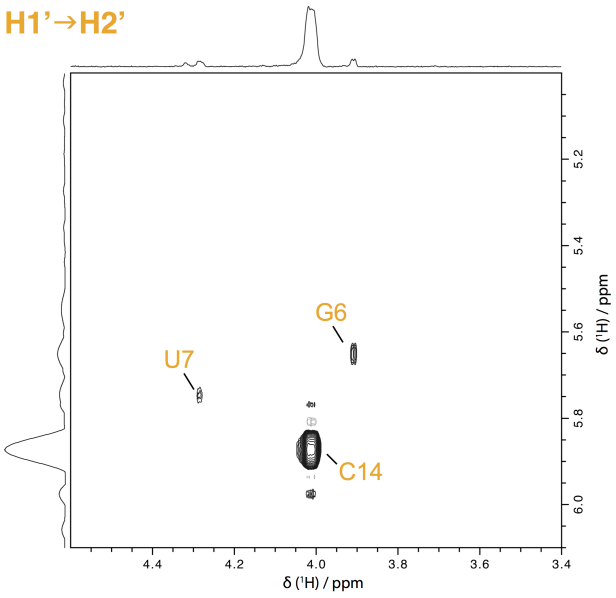

1.4 2D SELOPE spectra for GUC

1.4.1 H8/H6-H5 2D and HSQC for comparison

Figure S04 shows the diagonal of the H8 / H6-H5 2D spectrum of GUC. The H6-H5 cross peak region is shown in Figure S05.

Figure S04

^{1}H-^{13}C HSQC of the GUC RNA construct including assignment. 128 scans were recorded per increment (number of increments = 256 for SW = 30 ppm) with a recovery delay of 1.5 s leading to an overall experimental time of 15 h 17 min.
The spectrum is overlaid with the projection of the H8 diagonal of the H8/H6-H5 2D spectrum to show the depletion effect.

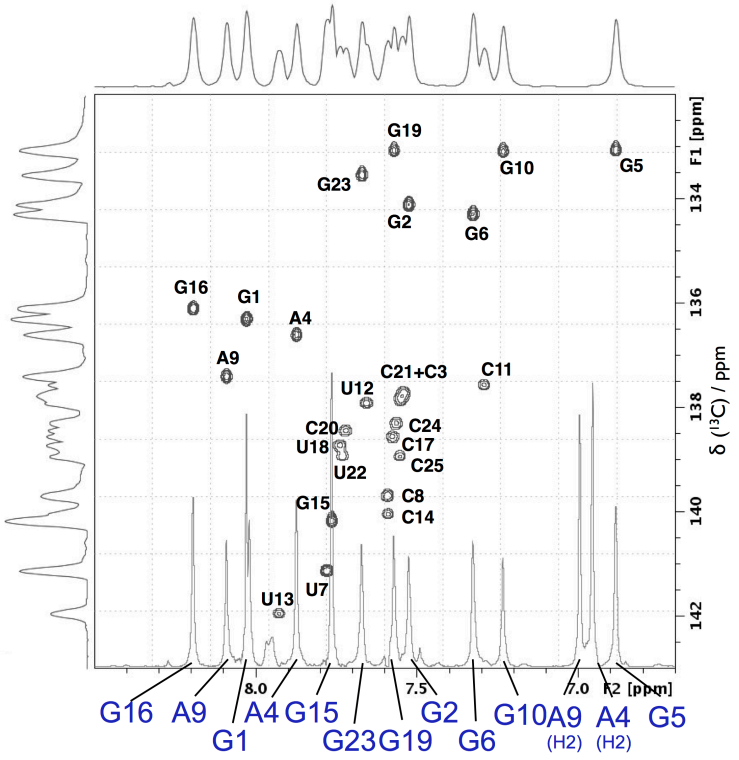

Figure S05

H6-H5 region of the acquired 2D H8/H6-H5 spectrum of GUC. Using a τ delay optimized to fully transfer H5 magnetization to H6. For this spectrum 44 FIDs were recorded for an indirect dimension of 1.8 ppm spectral width. 16 scans were recorded per increment with a recovery delay of 1.5 s leading to an overall experimental time of 27 min.

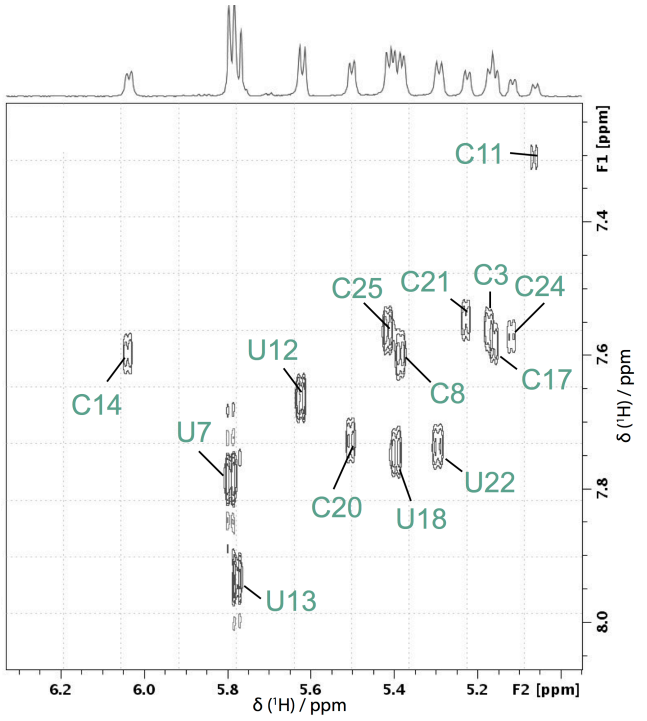

1.5 2D SELOPE for HBV ε apical stem-loop

A further RNA we studied, using the SELOPE technique, is the 27nt apical stem-loop of the hepatitis B virus (HBV) (Figure S06c). Figure S06 (a) shows the diagonal of the H8 / H6-H5 2D spectrum. The H6-H5 cross peak region is shown in Figure S06 (b).

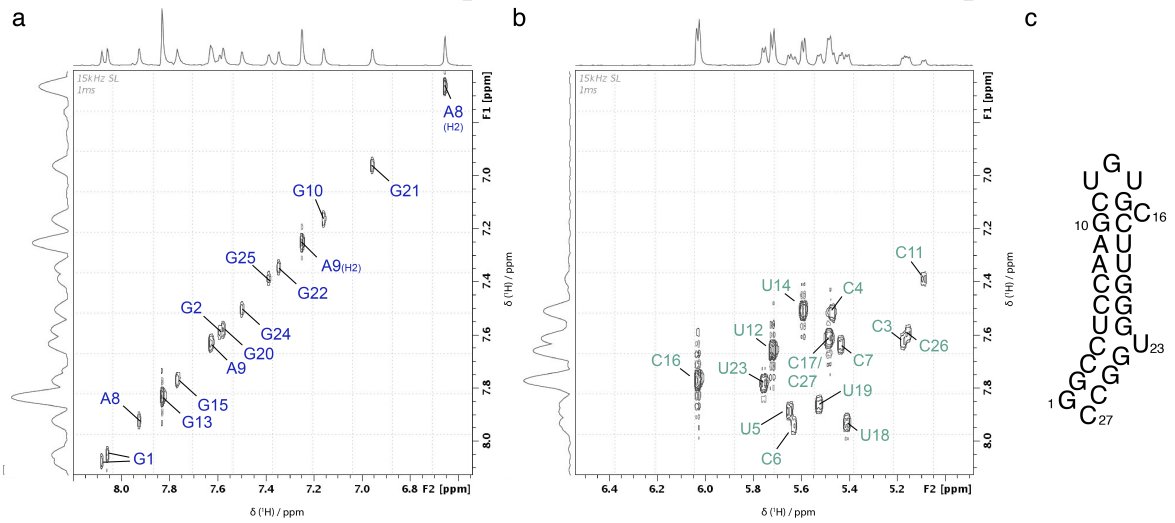

Figure S06. (a and b) H8/H6-H5 spectrum of the HBV construct. 40 FIDs were recorded for an indirect dimension of 1.55 ppm spectral width. 32 scans were co-added with a recovery delay of 1.5 s leading to an overall experimental time of 51 min. The sample concentration is ~1mM. (c) Secondary structure of the HBV construct as proposed in [7].

The spectra were assigned based on [7]. A comparison of the HSQC spectrum[7] with the de-crowded H8/H6-H5 spectrum shows that in this case the peaks are better dispersed with the proton nucleus in the indirect dimension than when using carbon. It can be seen that the 2D SELOPE idea clearly opens up the possibility to study structure and dynamics of this biologically interesting construct.

1.6 2D SELOPE for labeled RNAs

The new experiment can also complement other 2D experiments usually carried out with ^{13}C in the indirect dimension. Due to the depletion effect and the different indirect dimensions a proton peak can be well resolved in the selective ^{1}H-^{1}H 2D experiment, while it is overlapped in the heteronuclear correlation spectrum and vice versa. While this pulse sequence was mainly developed for unlabeled samples, we also present a modified version of the pulse sequence (see Figure S07), which can be applied to labeled RNA samples and a spectrum obtained for ^{13}C, ^{15}N labeled GUC (see Figure S08).

Figure S07

Selective ^{1}H-^{1}H pulse sequence with ^{13}C and ^{15}N decoupling for measurement on labeled RNAs.

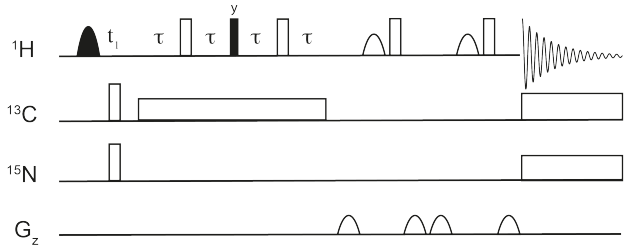

Figure S08

H6-H5 region of the acquired 2D H8/H6-H5 spectrum of labeled GUC. Using a τ delay optimized to fully transfer H5 magnetization to H6. For these spectra 50 FIDs were recorded for an indirect dimension of 1.4 ppm spectral width. 16 scans were recorded per increment with a recovery delay of 1.5 s leading to an overall experimental time of 26 min. Garp decoupling was applied on both, ^{15}N and ^{13}C during acquisition and on ^{13}C during the *J*-transfer.

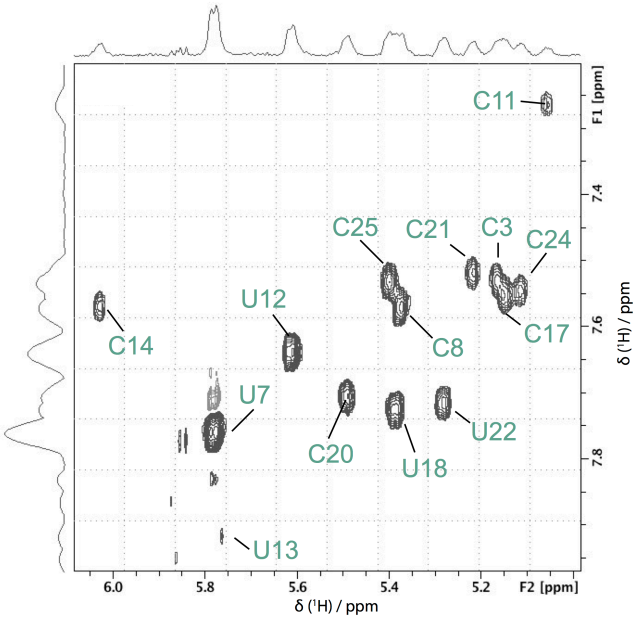

2. SELOPE $R_{1\rho}$ RD

2.1 Pulse sequence and experimental details

The selective ^{1}H-^{1}H 2D pulse sequence, modified to include a spinlock (SL) to measure relaxation dispersion (RD) is shown in Figure S09.

Figure S09
Selective ^{1}H-^{1}H 2D pulse sequence with selective excitation and SL for RD measurements.

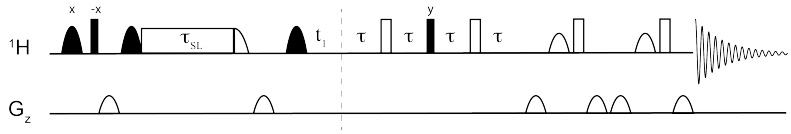

The ^{1}H frequency carrier is centered on the resonance of a single peak or multiple peaks of interest at the beginning of the experiment. Selective magnetization is created before the spin lock using a selective 90(x) – hard 90(-x) element followed by a purge gradient. As described for the original 2D experiment, for selective excitation of the H8/H6 region of the proton spectrum 4 ms Eburb2 shaped pulses[1] were used. The magnetization is then aligned along the effective field where it is spinlocked by a square pulse for variable durations τ_{SL} at the desired power level. It is then rotated back to the z-axis by a time-reversed tanh/tan adiabatic ramp as used in the previously published experiment for labeled samples[8]. As presented in the original selective 2D experiment (see main manuscript Fig 2a and section 1.2 of this supplementary), the remaining magnetization is then brought to the xy-plane for the indirect evolution time t_1 before undergoing the *J*-transfer step.

Relaxation dispersion experiments in this work were carried out as 2Ds as well as 1Ds, depending on the sample, proton of interest and SL strength. In the following sections of this SI, we present relaxation dispersion results obtained for various protons in two different samples (GUG and GUC, secondary structures indicated in the main paper, Figures 3 and 4). Further experimental details and whether the data was extracted from 1D or 2D data sets are mentioned there.

2.2 $R_{1\rho}$ processing and data analysis

$R_{1\rho}$ values were extracted from exponential fits of deconvolved peak intensities from 1D or 2D data sets and ^{1}H RD curves were then fitted to two-state fast exchange limit equations as described in Ref.[8].

2.3 SELOPE $R_{1\rho}$ GUG

The 25nt GUG RNA construct was selected to demonstrate the ability of the presented sequence to measure exchange processes beyond 50 kHz. In this case SL strengths between 1.5 and 15 kHz were used. For each strength five 2D spectra were recorded with τ_{SL} set to 1, 20, 60, 110 and 149 ms, respectively. The carrier frequency was set in the middle of the region of interest (H8/H6) to 7.5 ppm. For these spectra 44 FIDs were recorded for an indirect dimension of 1.8 ppm spectral width. 32 scans were recorded per increment with a recovery delay of 1.5 s leading to an overall experimental time of 54 min per spectrum. This way it was possible to obtain dispersion curves for each H8 and H6, meaning each base within the whole RNA molecule, from one set of experiments (4.5 h). Intensities were

extracted using the dcon2D function on Bruker Topspin and data fitted as described under 2.2.
Figure S10 shows an overview comparing the exchange contributions observed for all nucleotides (H8/H6) and base pairs (NH) in this sample.

Figure S10

Overview of the whole GUG construct with darkest shades indicating nucleotides and base pairs exhibiting highest relaxation dispersions while lightest shades indicate no dispersion on this base.

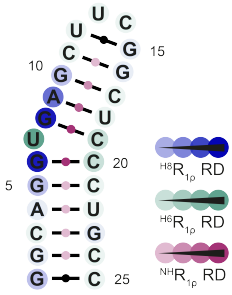

2.3.1 $R_{1\rho}$ GUG H8/H6 dispersion curves and fits

Relaxation dispersion curves for H8 and H6 (read out on H5) protons are shown in figures S11 and S12, respectively. For off-resonance artifacts as observed on e.g. G16 and G1, see 2.7.1.

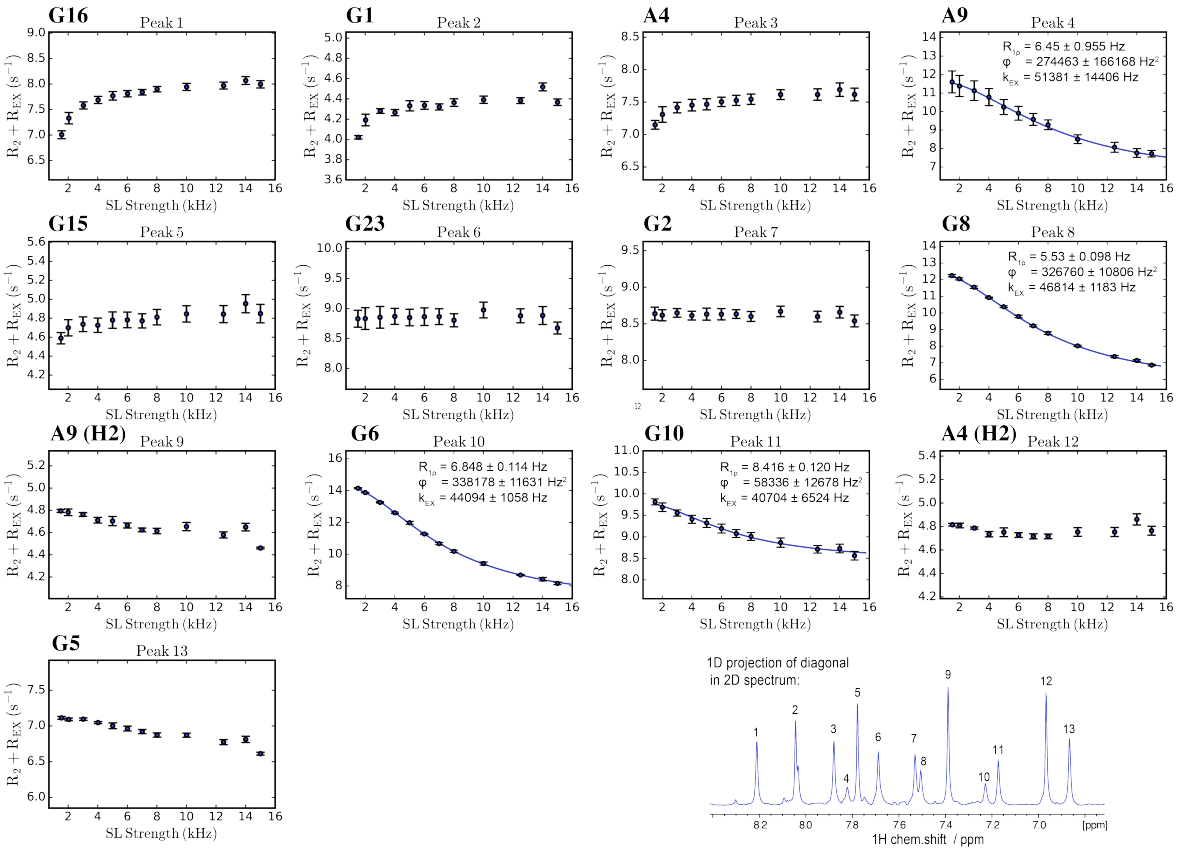

Figure S11. On-resonance H8 relaxation dispersion curves for GUG including fits for residues with significant, fittable exchange contributions.

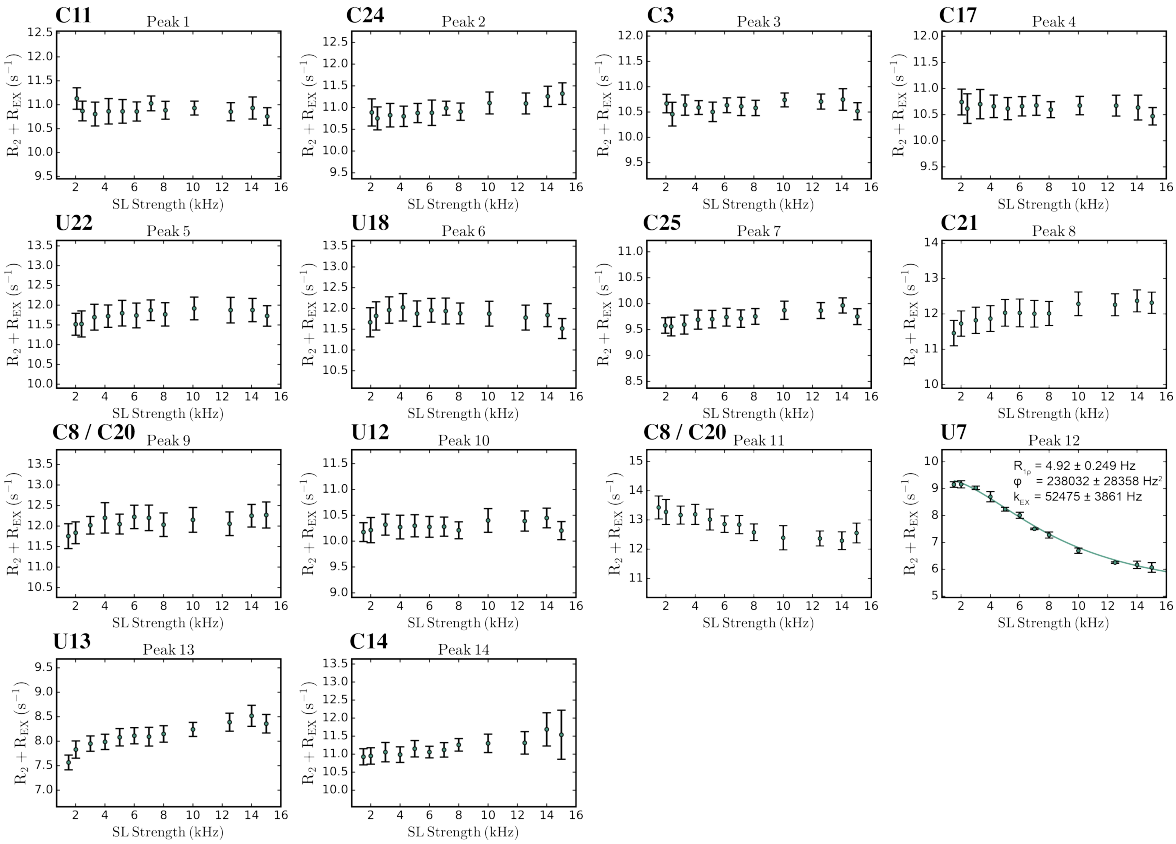

Figure S12. On-resonance H6 RD curves read out on H5s including fits for residues with significant, fittable exchange contributions.

2.3.2 $R_{1\rho}$ GUG NH dispersion curves and fits

For completion to fully study the GUG construct, 1D ^{1}H(N) $R_{1\rho}$ measurements were carried out. The imino proton signals are dispersed enough in the 1D spectrum (see Fig. S13), therefore the pulse sequence was modified to a simple 1D spinlock sequence, omitting the *J*-transfer element as shown in Fig. S14.

Figure S13

Imino ^{1}H region of a 1D spectrum of GUG. The peak numbering refers to the dispersion curves in Figure S14.

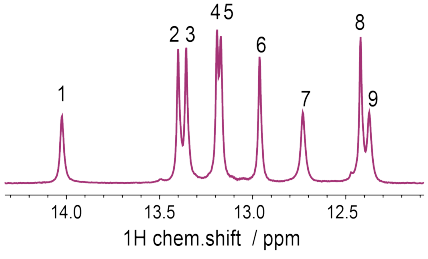

Figure S14

1D ^{1}H RD pulse sequence used for NH protons. In this case a 2 ms EBurp2 shaped pulse was used, o1 was set to 13.1 ppm.

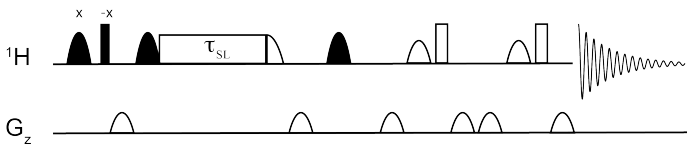

As for the H8/H6 experiment SL strengths between 1.5 and 15 kHz were used. For each strength 8 1D spectra were recorded with τ_{SL} set to 1, 5, 10, 20, 30, 40, 60 and 80 ms, respectively. Figure S15 shows dispersion curves and fits obtained for all detectable NHs in GUG. For off-resonance artifacts as observed on e.g. U18 and G23, see 2.7.1.

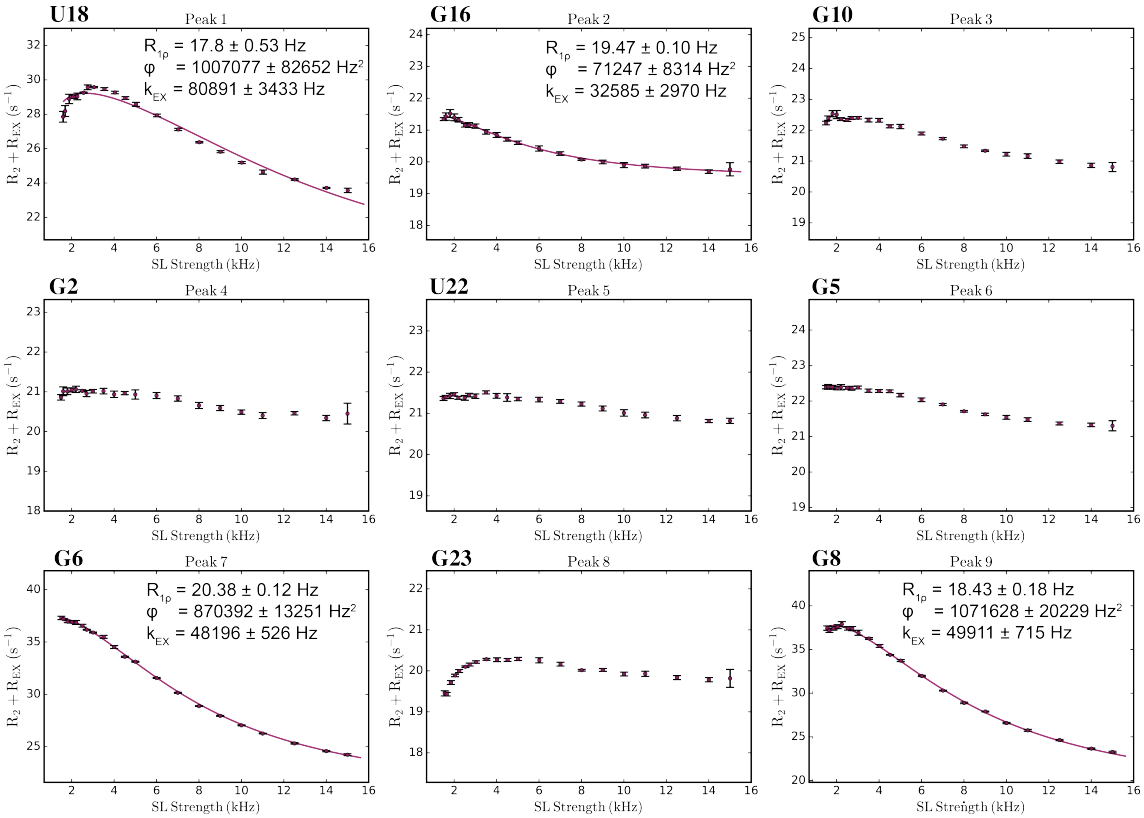

Figure S15. On-resonance NH RD curves including fits for residues with significant exchange contributions.

2.3.3 $R_{1\rho}$ GUG, titration with Mg^{2+}

To mimic physiological changes and monitor the system's response we have titrated the sample with $MgCl_2$ and acquired the same set of spectra as described in section 2.3.1 and 2.3.2. Figure S16 and Table 1 in the main text show results of the RD measurements for residues in the dynamic bulge region.

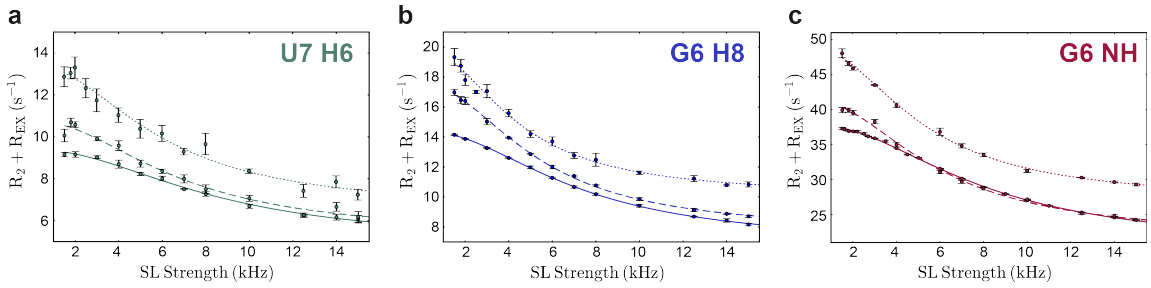

Figure S16. On resonance ^1H $R_{1\rho}$ relaxation dispersion data for an H6 (a), H8 (c) and NH (d) including best fits to a two-state fast exchange model obtained for the pure GUG sample (solid lines) as well as the sample titrated with $MgCl_2$ (6 mM, and 12 mM Mg^{2+} concentration shown as dashed lines and dotted lines, respectively).

2.3.3.1 GUG, titration with Mg^{2+}, chemical shift perturbation (CSP)

It should be mentioned that using the 2D spectra it is also possible to monitor chemical shift changes upon titration. As an example we show chemical shift changes obtained for H8 (Fig. S17) and H6 (Fig. S18) protons in the GUG construct at 0, 2, 6 and 12 mM Mg^{2+} concentration. An overview for the whole GUG construct is shown in Figure S19, below. It can clearly be seen that for the titration with Mg^{2+} the changes in chemical shift do not correlate with the changes in dynamics. (*e.g.* U7 does not undergo changes in chemical shift, while its dynamics change significantly upon Mg^{2+} titration.)

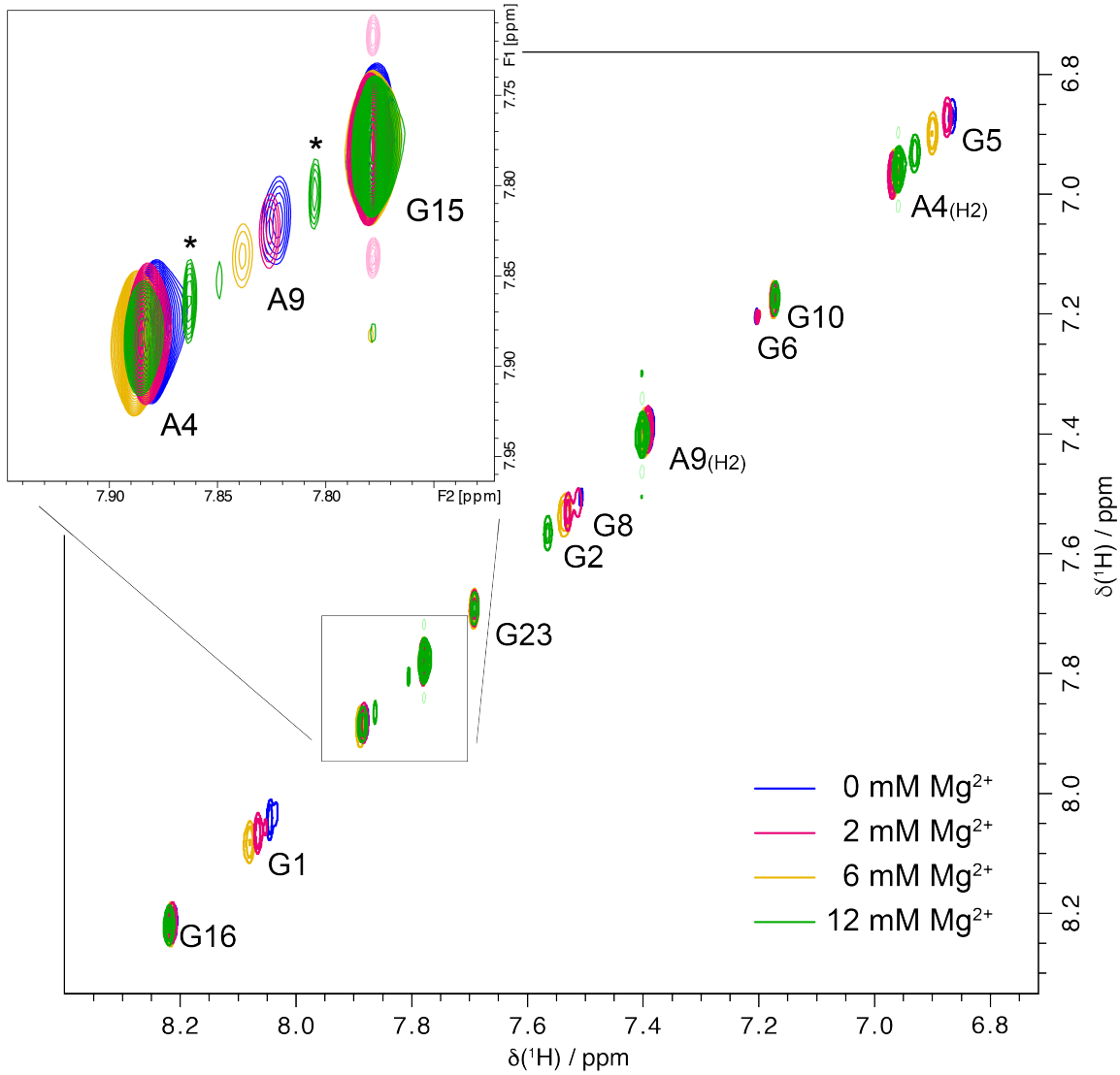

Figure S17. H8 region of the acquired 2D H8/H6-H5 SELOPE spectra (since we recorded $R_{1\rho}$ data anyway, in this case we used $R_{1\rho}$ spectra with 15 kHz SL, 1 ms data point) of labeled GUG. The overlay shows the pure GUG sample (blue) as well as the sample titrated with $MgCl_2$ (2 mM (red), 6 mM (yellow) and 12 mM Mg^{2+} concentration (green)). Expansion shows lower contour levels, allowing the visualization of A9 (lower intensity).

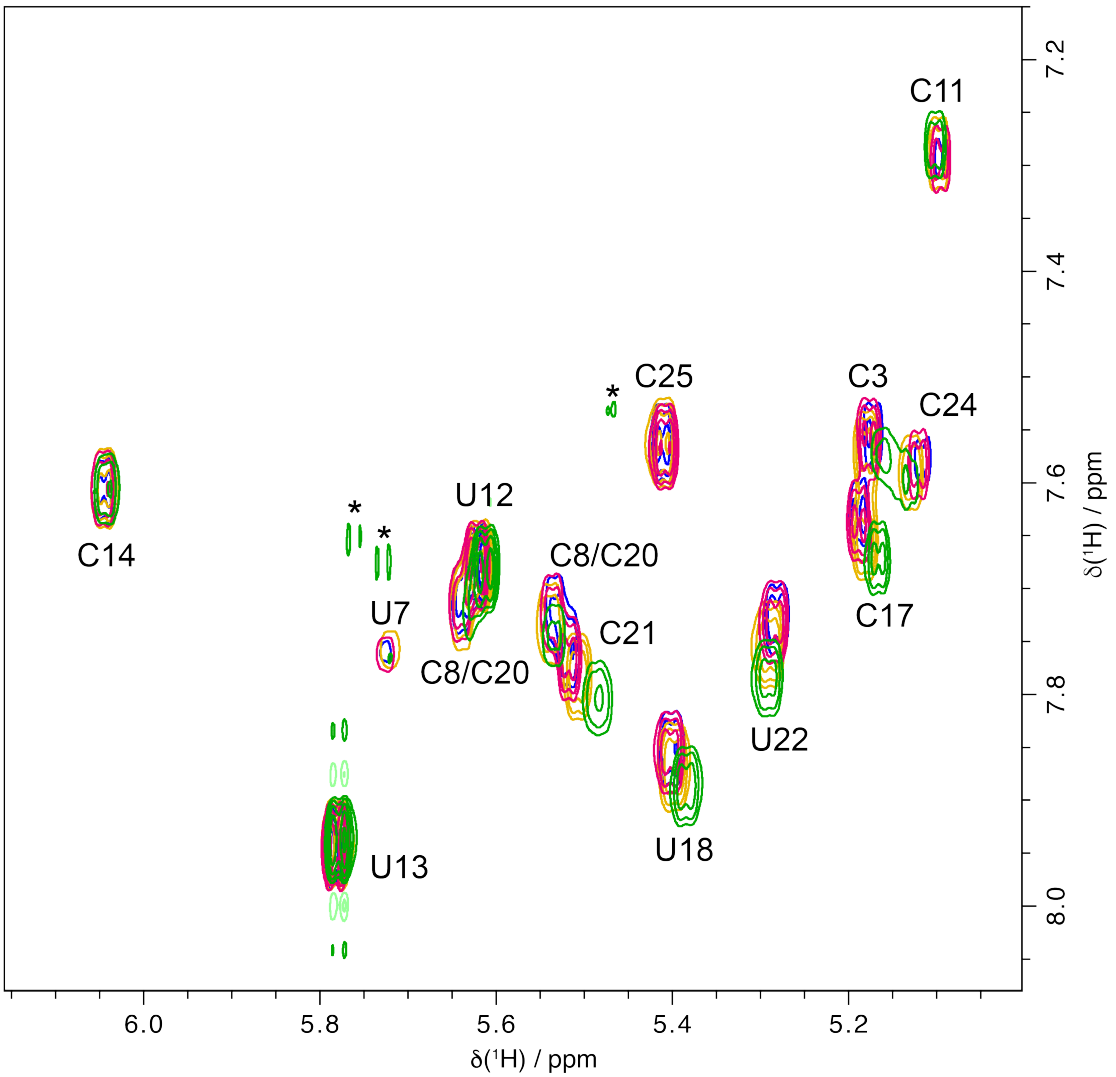

Figure S18. H6-H5 region of the acquired 2D H8/H6-H5 $R_{1\rho}$ spectra (15 kHz SL, 1 ms data point) of labeled GUG. The overlay shows the pure GUG sample (blue) as well as the sample titrated with $MgCl_2$ (2 mM (red), 6 mM (yellow) and 12 mM Mg^{2+} concentration (green)).

Figure S19

Overview of the whole GUG construct with darkest shades indicating residues exhibiting highest chemical shift perturbations upon Mg^{2+} titration, while lightest shades indicate no chemical shift change on this base.

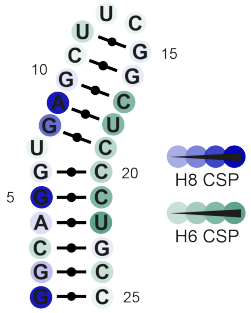

2.3.4 $R_{1\rho}$ GUG, titration with Neomycin

This method can also be beneficial to use unlabeled RNA samples for drug screening by monitoring changes in the dynamics of the system upon interaction with a drug molecule. As an example we have added a commonly used aminoglycoside, Neomycin, to the investigated NMR sample. Especially in the imino region of the spectrum changes of the dynamics (particularly from the G6-C20 base pair upwards to C11-G16) could be observed indicating incorporation of the drug into the helical structure influencing the Watson Crick base pairing.

Figure S20
Relaxation dispersion data for G6 NH (a) and G16 NH (b) of the pure GUG sample (purple circles) as well as after addition of Neomycin (green crosses). Solid lines are best fits to a two-state fast exchange model.

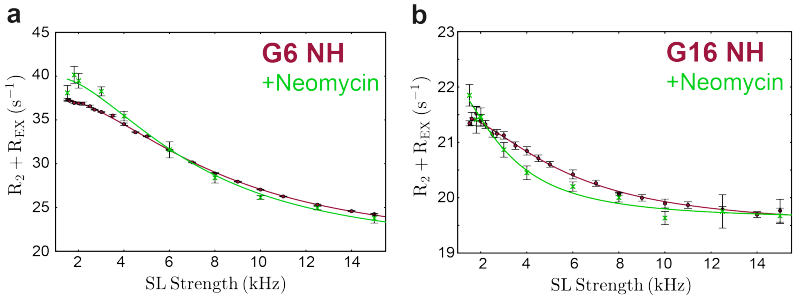

Fits to a two state fast exchange model result in $k_{EX}^{GUG} = 48496 \pm 523$ Hz and $k_{EX}^{NEO} = 41929 \pm 4393$ Hz for G6 NH without and with Neomycin, respectively, and $k_{EX}^{GUG} = 32585 \pm 2778$ Hz and $k_{EX}^{NEO} = 16887 \pm 3261$ Hz for G16. This indicates that Neomycin slows down the present exchange process.

2.4 SELOPE $R_{1\rho}$ GUC

The 25nt GUC RNA complex was selected to demonstrate the ability of the presented sequence to measure slower exchange processes. In this case SL strengths between 25 Hz and 4 kHz were used. The pulse sequence shown in Figure S09 was modified with a hard pulse replacing the ramp after the SL since the adiabatic condition would not be fulfilled for the low SL powers used. (It should be noted that even though we decided to only run these experiments up to 4 kHz SL strength, it is definitely possible to continue to run experiments up to 15 kHz using the same pulse sequence.) Due to the low power SLs, the carrier frequency was set to the chemical shift of the peak of interest and a set of six spectra with τ_{SL} set to 1, 20, 40, 60, 110 and 149 ms, respectively for each SL strength was recorded separately for each peak of interest. To keep the measurement time efficient, in case of all studied H8s, the pulse sequence shown in Fig S09 was run as a 1D with 48 or 64 scans leading to experiment times from 2-3 min per data point in the exponential decay. (The 1Ds for one SL strength were grouped and set up as a pseudo-2D with varying SL duration in the indirect dimension). In case of the H6 protons, if overlap in the 1D was small enough to allow deconvolution 1D spectra were used. Only for protons, which showed severe overlap in the 1D, the sequence was run as a 2D but with a very small SW in the indirect dimension, just making sure that no signal folds on top of the signal of interest. (*e.g.* for C8, the carrier was set to the chemical shift of H6(C8) and 10 FIDs were acquired for an indirect dimension of 0.4 ppm with 16 scans each, leading to an experiment time of ~6 min per data point in the decay curve). Intensities were extracted using the "multidcon" or "dcon2D" function on Bruker Topspin and data fitted as described under 2.2.

2.4.1 $R_{1\rho}$ GUC H8/H6 dispersion curves and fits

A set of representative on-resonance relaxation dispersion curves for a few H8 and H6 (read out on H5) protons are shown in Figures S21 and S22, respectively.

Figure S21
^{1}H $R_{1\rho}$ RD data for H8 of A4, G6, and A9. Solid lines are best fits to a two-state fast exchange model.

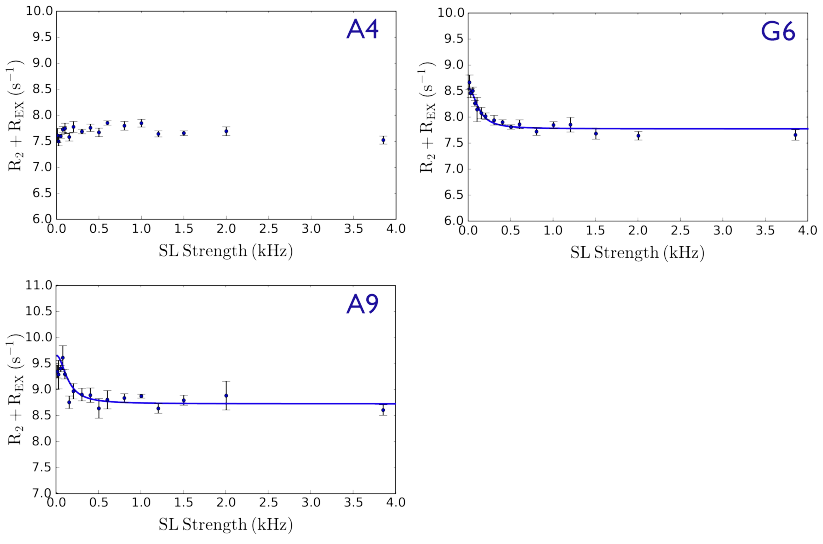

Figure S22
^{1}H $R_{1\rho}$ RD data for H6 of U7, obtained from 1D spectra and C8, obtained from a set of 2Ds.

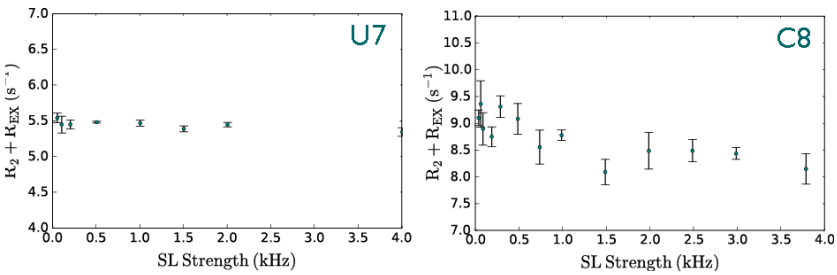

2.5 SELOPE $R_{1\rho}$ off-resonance measurements GUC

To show the ability of the developed sequence to obtain chemical shift information as well as populations of the excited state, off-resonance RD measurements were carried out on the GUC construct. To record off-resonance data the pulse sequence shown in Figure S08 was modified with hard pulses with adjustable flip angles replacing the selective pulse and ramp before and after the SL. A frequency shift command was implemented to allow variable off-resonance SLs. See also Reference[8].
In addition to the off-resonance profile for G6, presented in the main article in Figure 4, Figure S23 shows an off-resonance profile for H8 of A9. Fittings were obtained solving the Bloch-McConnell equations for two-state chemical exchange[9]. Results for both residues are shown in Table S1.

Figure S23
^{1}H $R_{1\rho}$ off-resonance RD data for H8 of A9. Fitted parameters are shown in Table S1.

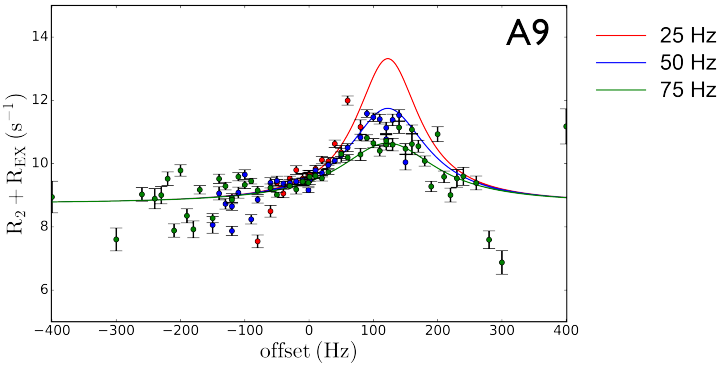

Table S1 Fitting results for the presented residues.

	R_1 / Hz	R_2 / Hz	k_{EX} / Hz	p / %	$\Delta\omega$ / Hz
G6	2.84 ± 0.01	7.99 ± 0.05	263 ± 30	0.40 ± 0.03	–111 ± 5
A9	3.34 ± 0.01	8.97 ± 0.07	322 ± 41	0.38 ± 0.04	121 ± 6

2.6 SELOPE $R_{1\rho}$ H44 top

We compared our new method to the recently published method to measure proton RD on labeled RNA samples[8]. Figure S24 shows data obtained using the two different methods for the H44 top construct as studied in ref[8]. The data obtained using SELOPE on the unlabeled construct (red dots) is showing an additional excited state in the slow exchange regime, which was inaccessible when using the previous method[8] on the labeled sample (blue dots). In addition, R_2 values in unlabeled samples are lower leading to less noise in R_2 + R_{ex} data and therefore higher sensitivity of the SELOPE approach.

Figure S24
^{1}H $R_{1\rho}$ on-resonance RD data for H2 of A18 in H44 obtained from an unlabeled sample using the SELOPE approach (red circles) and a labeled sample using the method presented in ref[8]. This shows the wide range of dynamics accessible due to a SL range of 50 Hz to 15 kHz available in the SELOPE approach.

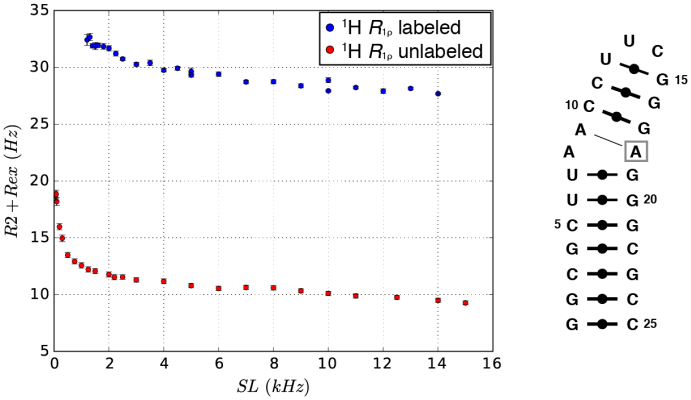

2.7 $R_{1\rho}$ Artifacts

2.7.1 Off-resonance effects in on-resonance data sets

In case of on-resonance RD experiments carried out in a time-saving 2D way (obtaining information on all residues in one experiment, as done for GUG) off-resonance effects are visible for peaks furthest away from the carrier frequency of the SL. This is especially the case for lower SL strengths (1.5 - 4 kHz). The effect can be seen in Figures S10-S13 for peaks with biggest offsets as an increase of $R_{1\rho}$ for SLs between 1.5 and 4 kHz. To account for this effect we do not assume $R_{1\rho} = R_2$ in the fitting protocol, but account for the off-resonance effect by calculating the effective field angle theta (depending on the chemical shift of the peak of interest with respect to the SL carrier and the SL strength) to calculate $R_{1\rho} = R_1 \cos(\theta)^2 + R_2 \sin(\theta)^2$. Figure S25 shows a simulated RD curve assuming no exchange with off-resonance effect, using offset-values and R_2 values of NH of G23. The experimental curve for this residue can be found in Figure S15.

Figure S25
Simulated offset effect for NH of G23, with R_2=21Hz and R_1=3Hz (blue dots), R_1=5Hz (green crosses) and R_1=0Hz (red crosses). The different R_1 values were chosen to show the influence of R_1. In practice to fit on-resonance RD curves with k_{EX} for NHs, the R_1 dependent term of the equation was neglected, since R_1 is usually not known and the off-resonance contribution is smaller compared to R_2.

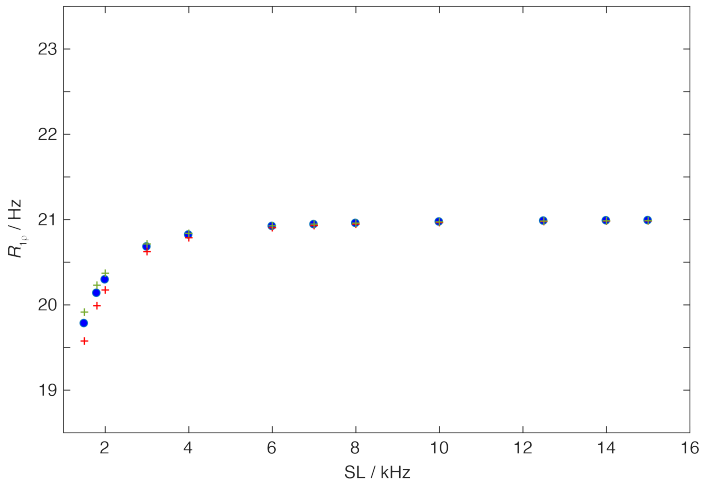

2.7.2 Heating effects

With SLs over a range of 25 Hz up to 15 kHz for durations of up to 150 ms, heating effects are clearly visible in form of small chemical shift changes. To even out those effects a standard heat compensation for the duration of the SL is carried out far off-resonance (-100 kHz) as described in Reference[8]. An additional heat compensation element was introduced to even out effects arising due to different SL strengths. Therefore a second heat compensation block was introduced with an additional far-off-resonance SL carried out at a compensating SL strength. This additional heat compensation element can be omitted if all data sets are acquired at once and scans for different SL strengths are acquired in interleaved and randomized ways.

2.7.3 Hartmann-Hahn cross polarization

A typical relaxation dispersion curve with artifacts arising due to Hartmann-Hahn cross polarization[10] is shown in Figure S26, middle panel.

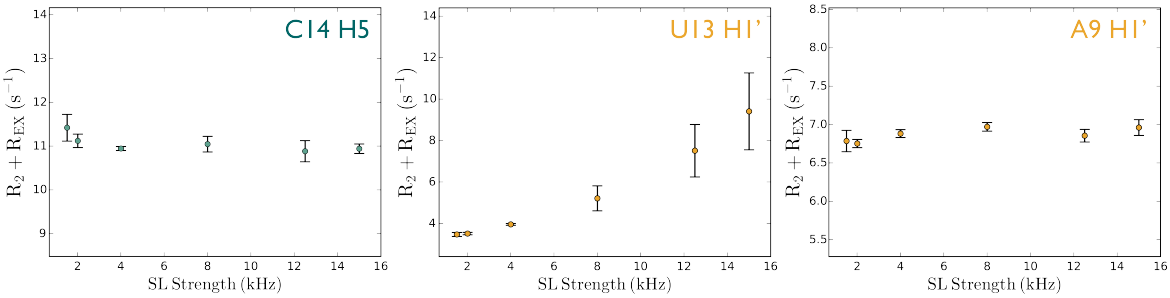

Figure S26. On-resonance ^{1}H $R_{1\rho}$ RD data for H5 of C14, H1' of U13 and A9 obtained from 1Ds.

For H6/H5 and H1'/H2' spin pairs, special care has to be taken when setting the spinlock carrier to avoid Hartmann Hahn matching conditions. This is especially a problem when running the ^{1}H RD experiment as an 2D, when the spin of interest is off-resonant regarding the SL carrier to the opposite side as the spin it is coupled to. In case of high power SLs even if the SL carrier is not equidistant to the two coupled spins, the effective fields are similar enough to allow a coherence transfer. This manifests itself as apparent increase in R_2+R_{EX} values with increasing SL strength, as can be seen in Figure S26 for H1' of U13.
As comparison, we have added RD curves obtained for two other residues from the same data set, where the SL carrier frequency is not as "unfortunate" with respect to the chemical shift differences (see C14 H5, Fig. S26 left panel) and the *J*-coupling constant is small (see A9 H1', Fig. S26 right panel).

A closer look at the exponential decays (Fig. S27) for each RD data point for U13 shows an oscillation on top of the standard decay for high SL strengths. This can be used to identify the source of error and such decays should be omitted.

Figure S27

Relative signal intesities obtained from 2D ^{1}H RD experiments for τ_{SL}= 1, 20, 40, 60, 110 and 149ms at different SL strengths for H1' of U13 including exponential fits.
It can be seen that in this case the error on the fitted parameter can be used as an indicator whether problems due to HH transfer will arise in the dispersion curves.

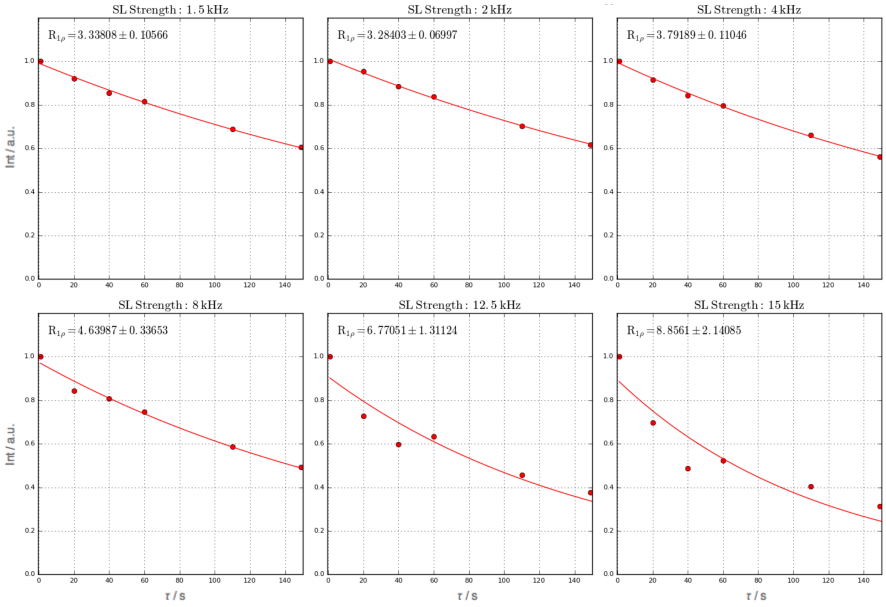

Simulations for high spinlock strengths with chemical shifts similar to the experimental values and typical *J*-coupling constants in C2' endo sugar conformation were carried out using SpinDynamica[11].

To test the influence on the exponential fitting, 6 data points for a 15 kHz SL were used for the simulated curves at SL durations τ = 0.001, 0.020, 0.040, 0.060, 0.110 and 0.149 s (these were also the used τ_{SL} in the experiments) for an exponential fit and compared the values to the actual $R_{1\rho}$ = 3.3 Hz used in our simulations. The values obtained from the exponential fit through these data points are $R_{1\rho,\text{ fit offres}}$ = 8.5 Hz in case the SL carrier is set between H1' and H2' ($\Omega_{H1'} = -2\pi$ 300 Hz, $\Omega_{H2'} = 2\pi$ 600 Hz, Fig. S28(a)) and $R_{1\rho,\text{ fit onres}}$ = 3.9 Hz for an experiment where the carrier is set on-resonance with respect to the spin of interest ($\Omega_{H1'} = 0$ Hz, $\Omega_{H2'} = 2\pi$ 900 Hz, Fig. S28(b)).

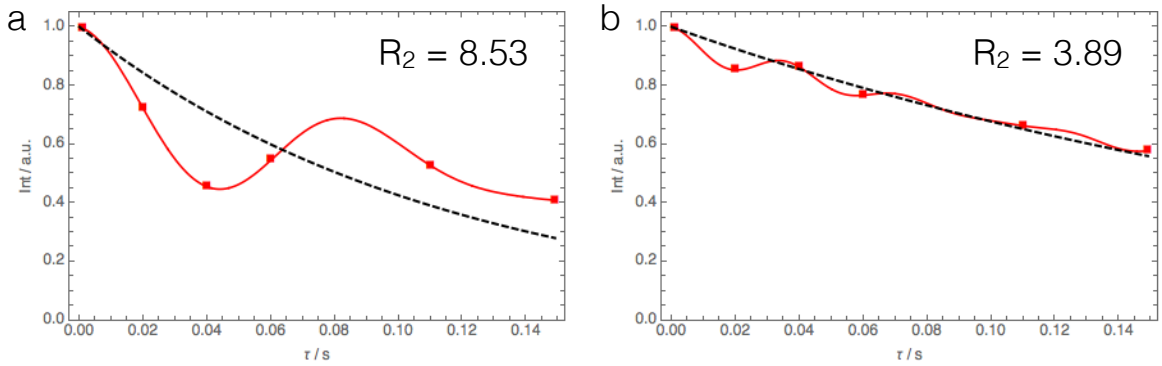

Figure S28. Simulated $R_{1\rho}$ relaxation curves for I_{1x} using the following parameters representative for H1's in C2' endo conformation: (a) $\Omega_1 = -2\pi$ 300 Hz, $\Omega_2 = 2\pi$ 600 Hz, $\Omega_3 = 2\pi$ 900 Hz, $\Omega_4 = 2\pi$ 600 Hz, $J_{12} = 8$ Hz, $J_{23} = 5.2$ Hz, $J_{34} = 1$ Hz, $\omega_{SL} = 2\pi$ 15000 Hz. (b) same as in (a) except $\Omega_1 = 2\pi$ 0 Hz, $\Omega_2 = 2\pi$ 900 Hz, $\Omega_3 = 2\pi$ 1200 Hz, $\Omega_4 = 2\pi$ 900 Hz. Dashed lines are exponential fits through the indicated simulated data points.

These results show that the error introduced in the case of on-resonance SL carrier settings are relatively small, even for very low R_2 values (as can be seen from the fitted R_2 value obtained in Figure S28b, which is closer to the theoretical value of 3.3 Hz which was used in the simulation). In addition, this simulation also shows that provided that chemical shifts and *J*-couplings were determined for the residue of interest, it is also possible to fit the exponential decay on top of the (then known) oscillation and therefore off-resonance experiments with "unfortunate" $\Delta\omega$ (where the excited state chemical shift lies between the chemical shifts of the two coupled spins) become available also for H1' and H5/H6 protons. (In this case one is advised to record more data points per exponential decay to allow for accurate fitting.)

2.7.4 Cross relaxation (ROE/NOE transfers)

Dipole-dipole based experiments (*i.e.* NOE) as used for assignment of RNAs show most intense cross peaks for H8-H1' and H6-H5 spin pairs. To determine the worst-case scenario of through space transfer during the SL for H8 and H6 protons, which could lead to artifacts in the relaxation dispersion measurement, we have measured ROE spectra using a 15kHz SL (the maximum SL used in the dispersion experiments). Figure S29-S31 show a selective ROESY spectrum as well as decay and build-up curves for a selection of residues of the GUG RNA construct.

Figure S29

^{1}H-^{1}H ROESY spectrum starting with selective excitation on H8/H6 region as used for RD experiments (same selective excitation and dephasing scheme, same carrier frequency) for a 149 ms 15 kHz SL. Display of the aromatic region of the spectrum.

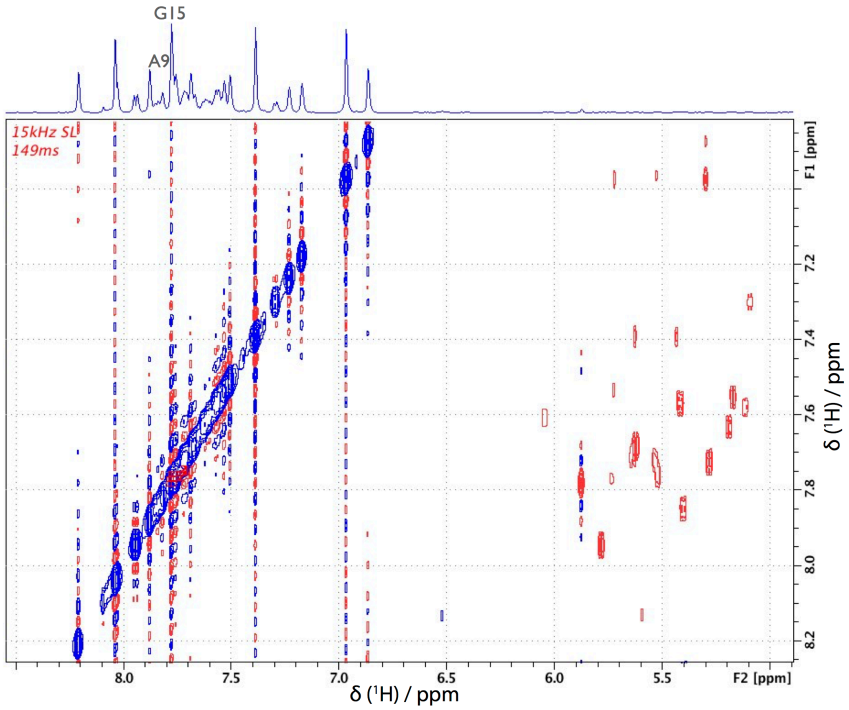

Figure S30

Decays and build-up curves for selected H8 and corresponding H1' peaks extracted from selective ROE experiments carried out with different SL durations (τ_{SL}). The SL frequency is 15 kHz.

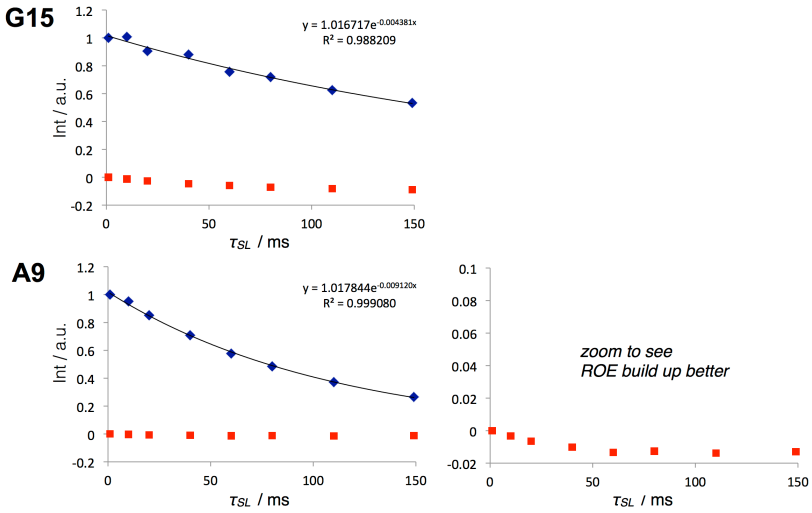

Figure S31

Decays and build-up curves for selected H6 and corresponding H5 peaks. The signal peak shape is indicated for H5 to the right of each build-up data point. For C17 and C14 the magnetization is transferred due to ROE and also due to Hartmann-Hahn matching.

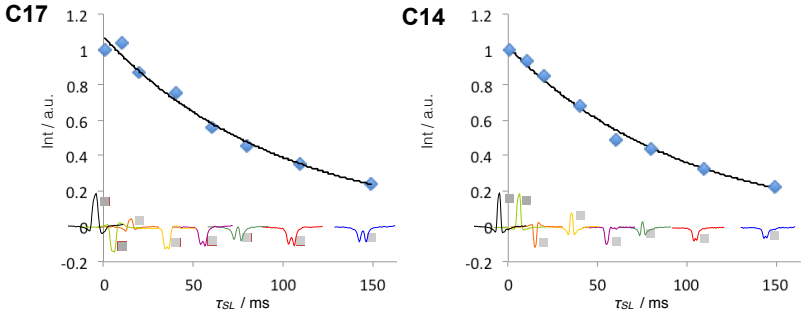

The above figures clearly show that a small amount of magnetization is transferred due to ROE during the SL. However, in case of GUG, where data was obtained for SL strengths between 1.5 and 15 kHz, RD curves are flat for residues where no exchange is expected. (See Figures S11 and S12). This clearly indicates that the influence of ROE on $R_{1\rho}$ values in the investigated range is negligible or constant within error, over the range of SL strengths used in this work. We therefore do not expect an influence (within error) on the exchange parameters extracted from those on-resonance $R_{1\rho}$ curves. Also in case of GUC, where we measured on-resonance curves with SL powers ranging from 25 Hz to 4 kHz, the influence of ROE on H8 seems to be within error of the experiment in our case (*e.g.* see residue A4 in Figure S21).
It should be noted that by using the pulse sequence with pulses with adjustable flip angle before and after the SL (as proposed in this publication for off-resonance measurements) it is also possible to adjust the angle of the effective field of the SL to 35.3º, and run a series of RD curves where cross-relaxation effects are compensated[12].

To determine the influence of cross-relaxation on off-resonance experiments as carried out on GUC for G6 and A9 (see Fig. 4 of the main text and Fig S22), we repeated the same measurement on A4, a residue without exchange and fitted it solving the Bloch-McConnell equations for two-state chemical exchange, as for the other residues.

Figure S32

^{1}H $R_{1\rho}$ off-resonance RD data for H8 of A4. Fitted results are:
R_1= 3.23 ± 0.02 Hz
R_2= 8.90 ± 0.15 Hz
k_{EX} = 51 ± 7 Hz
p = 0.27 ± 0.07 Hz
$\Delta\omega$ = –212 ± 43 Hz

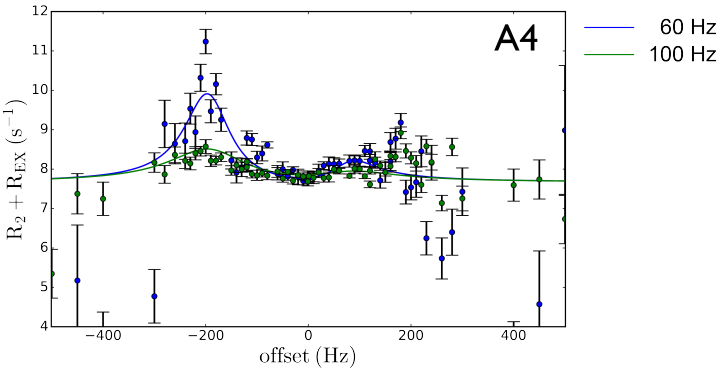

The off-resonance profile clearly shows a cross-relaxation artifact, which could be mistaken for an excited state. We decided to simply check for possible ROE/NOE candidates within our offset region of interest in a NOESY spectrum (see Figure S33). It can be seen that for A4H8 a NOE cross peak to C3H6 is visible. The chemical shift difference between those two peaks is 194 Hz (green arrow), indicating that the $\Delta\omega$ obtained from the off-resonance curve is due to ROE and not due to conformational exchange.

NOE cross peaks and chemical shift differences in the H8/H6 region of the NOESY spectrum are also indicated for A9 and G6 (pink arrows). In contrast to A4, $\Delta\omega$s obtained from fits of off-resonance curves for A9 and G6 (see Fig.4 of main text and Fig. S23) are not in the same range as chemical shift differences observed in the NOESY. These results show that in case off-resonance experiments are run it is recommended to check on a NOESY experiment what cross peaks are present and could cause ROE/NOE artifacts.

Figure S33
^{1}H-^{1}H NOESY spectrum as usually carried out for sequential assignment of RNA (mixing time 175 ms). Display of the aromatic region of the spectrum including sequential cross peaks indicated for some residues. The projection of F2 is overlaid with the projection of the selective 2D (in magenta), therefore only showing H8s.

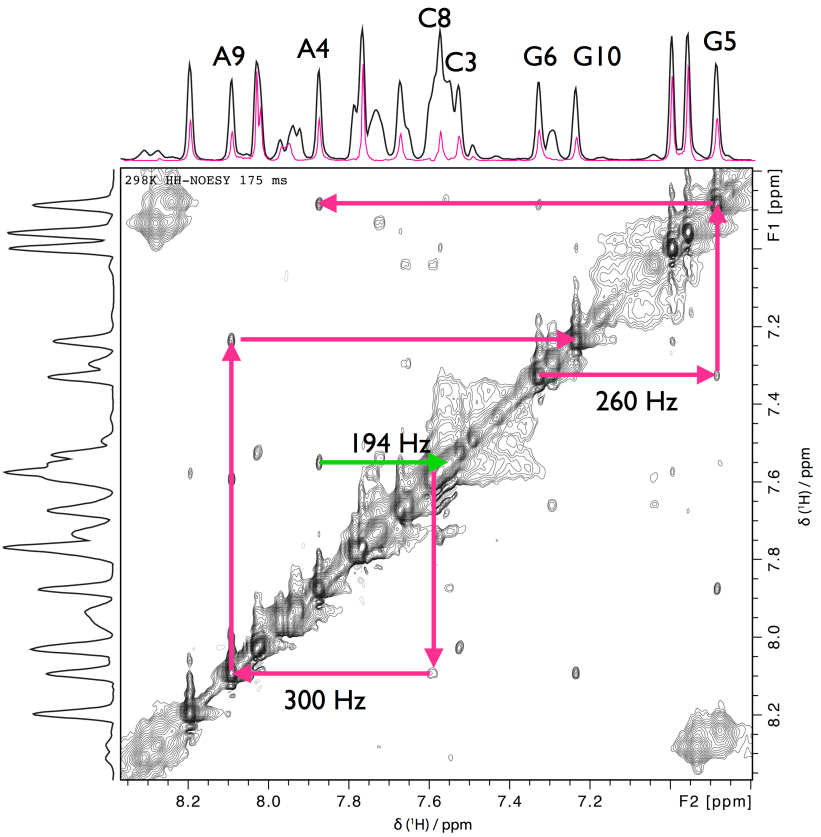

3. SELOPE CEST

3.1 Pulse sequence and experimental parameters

The selective *J*-transfer element can also be combined with a CEST[13] element. The pulse sequence is shown in Figure S34.

Figure S34
Selective ^{1}H-^{1}H pulse sequence with CEST element.

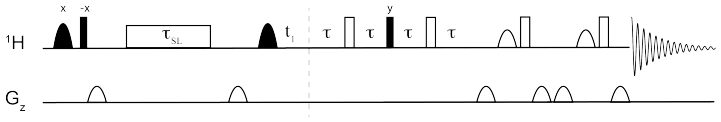

CEST experiments were carried out similar to $R_{1\rho}$ experiments (same experimental parameters for selective pulses etc.). A saturation duration of 400 ms was chosen except for the comparison experiment, where it was set to 0 ms.

3.2 SELOPE CEST GUC example

Exemplary CEST profiles obtained using this sequence are shown in Figure S35 and S36. Simulated curves (black lines) are obtained solving the Bloch-McConnell equations for two-site chemical exchange with the parameters derived from the ^{1}H $R_{1\rho}$ experiment reported in Table S1.

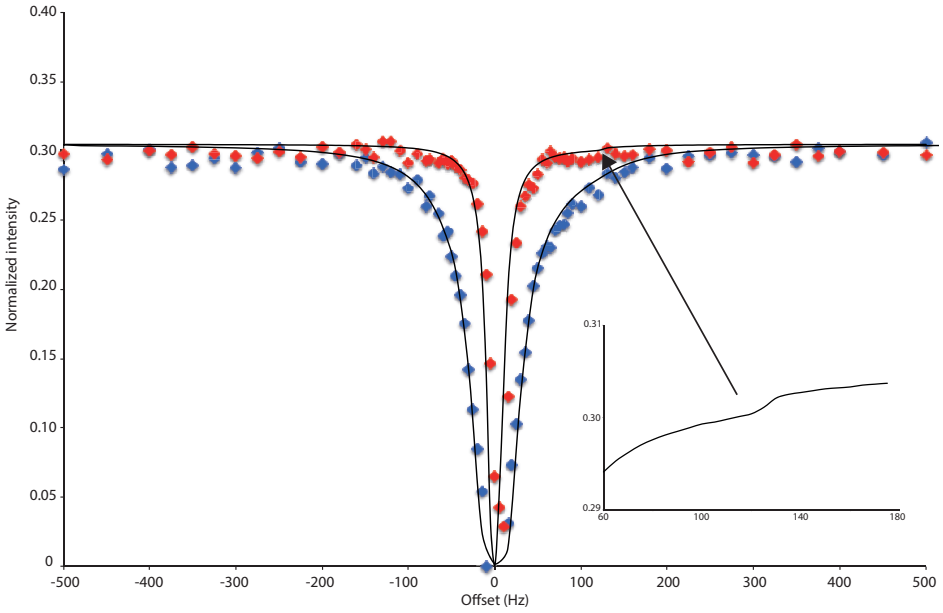

Figure S35. CEST profiles obtained for A9H8 using a 5 and 15 Hz SL, shown in red and blue respectively. The excited state which is clearly visible using the new ^{1}H $R_{1\rho}$ pulse sequence (Fig. S22 and Table S1) is barely visible when using CEST methodology (see insert showing a zoom of the simulated curve in the excited state region) demonstrating the power of the new method proposed.

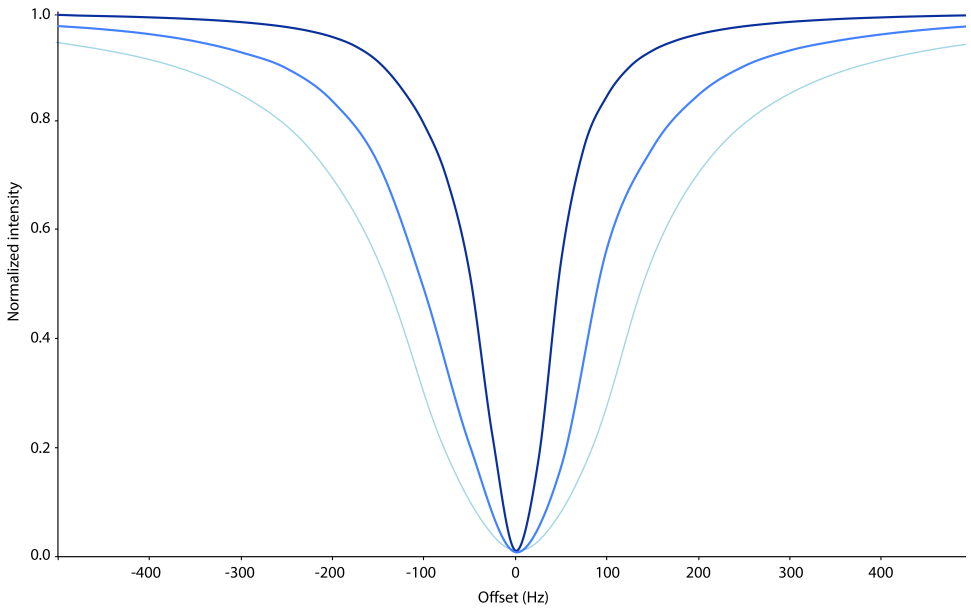

Figure S36. CEST profiles simulated for G6H8 using a 25, 50, 75 Hz SL, same color-coding as in the main article in Figure 4. The excited state, which is clearly visible using the new ^{1}H $R_{1\rho}$ pulse sequence (Fig. 4 in the main article and Table S1), is barely visible when using CEST methodology (as shown in this simulation).

4. SELOPE for DNA and Proteins

4.1 Experimental parameters and spectra for DNA

To show the potential of the presented technique for DNA we have applied the SELOPE approach to the Dickerson dodecamer d(CGCGAATTCGCG)$_2$ (purchased from IDT, 1.3 mM in NMR buffer (15 mM sodium phosphate, 0.1 mM EDTA and 25 mM NaCl at pH 6.5)). The experimental set-up was exactly the same as for the investigated RNA samples (see p. 1). The resulting H8/H6-H5 spectrum is shown in Fig. S37. As for RNA samples, in case of C-bases, the magnetization is fully transferred to H5 while for T-bases the magnetization is partially transferred from H6 to the CH3 group ($^4J_{HH}$ as indicated by the horizontal lines in Fig S37).

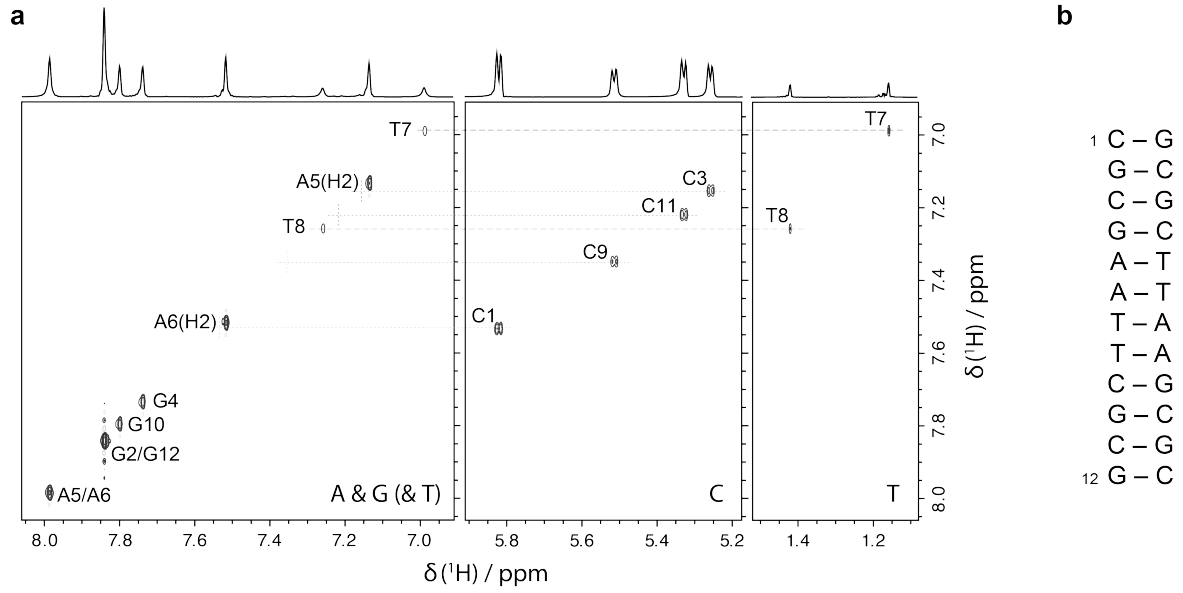

Figure S37. (a) H8/H6-H5 spectrum of the Dickerson dodecamer DNA sample. 16 scans were recorded per increment (number of increments = 80 for SW = 1.8 ppm) with a recovery delay of 1.5 s leading to an overall experimental time of 40 min. Assignment based on [14].

4.2 Experimental parameters and spectra for Proteins

To show the potential of SELOPE for protein NMR we have applied the pulse sequence on unlabeled Ubiquitin (2mM Ubiquitin in Na_2HPO_4/NaH_2PO_4 buffer, pH=5.6). In this case a 3ms Eburp pulse (carrier frequency was set to 4.2 ppm) was used for selective excitation of the Hα region and magnetization was transferred to NH. Due to the wider range of possible values for the $^3J_{H\alpha NH}$ coupling constant in proteins, compared to the RNA $^3J_{H5H6}$ couplings, we chose to use shorter transfer times (14ms) to ensure positive, absorptive line shapes for most peaks in the Hα-NH cross-peak region of the spectrum. As a consequence, there is hardly any depletion effect along the diagonal but for the majority of residues a significant amount of magnetization is transferred, hence they can be monitored via Hα-NH cross-peaks. Compared to a standard COSY experiment[15] all cross peaks are in-phase except those arising from Glycine residues.

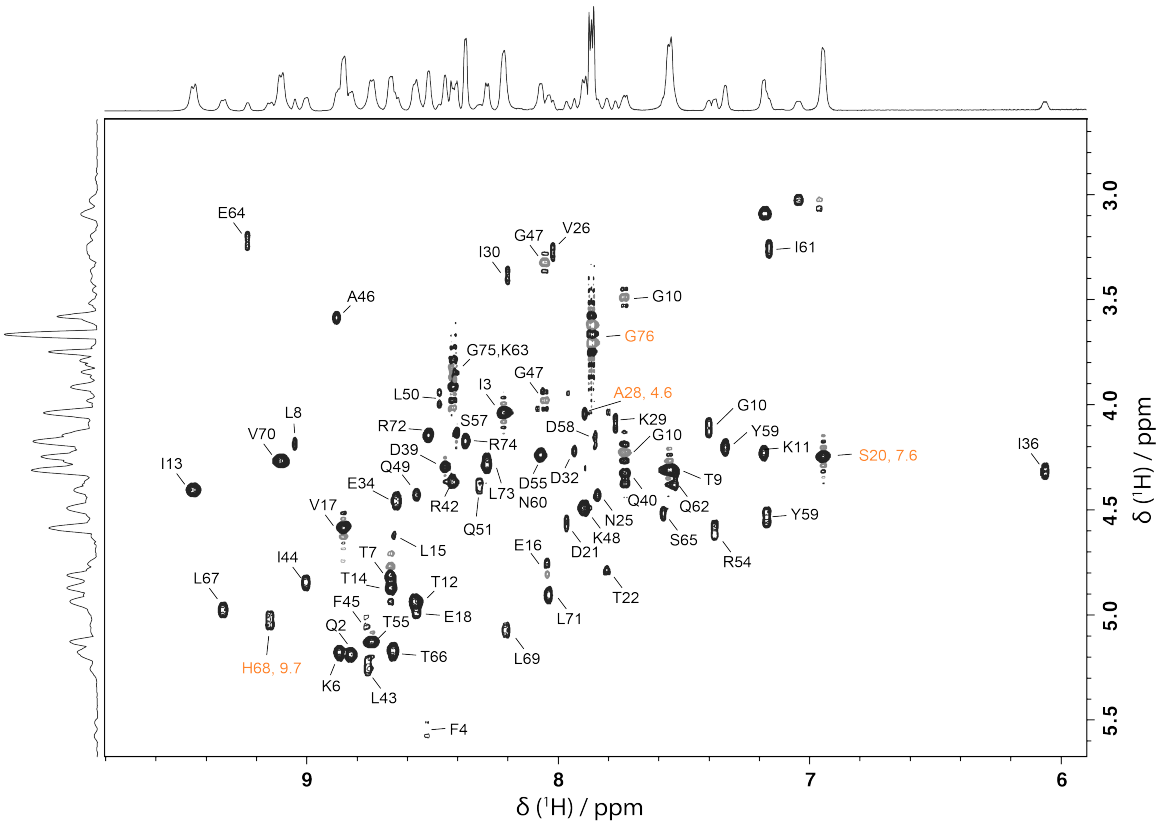

Figure S38. NH-Hα SELOPE of Ubiquitin. Representative residues are highlighted in orange: H68: ^{3}J=9.7 Hz (β-sheet), S20: ^{3}J=7.6 Hz (β-turn), A28: ^{3}J=4.6 Hz (α-helix), G76 (to point out lineshape of glycine signals). Peaks were assigned based on [15] and ^{3}J coupling constants were obtained from [16]. 48 scans were recorded per increment (number of increments = 128 for sw = 3.6 ppm) with a recovery delay of 1.5 s leading to an overall experimental time of 3 h 19 min.

5. SELOPE with TOCSY transfer

While it is not possible to achieve the complete selective transfer of one set of protons, and depletion of the region of the other set of protons, using a COSY type transfer as usually carried out in 2QF-COSY experiments, it is indeed possible to replace the "τ-180- τ -90- τ -180- τ" element with a TOCSY transfer. The optimum duration for the SL in that case is 1/(2*J*), which is 50 ms in the case of H5-H6 transfer.
Figure S39 shows an H8/H6-H5 spectrum acquired using a 50ms TOCSY transfer upon selective excitation. It can be seen that it also allows achieving the complete transfer of H6 to H5 and the depletion of the H8 region. This exploitation of the depletion effect in TOCSY for RNAs is shown for the first time here. When using the TOCSY transfer some residual NH_2 peaks (indicated by asterisks in Fig. S39) are visible in the depleted H8 region. These residual peaks are not visible in the normal SELOPE experiment since there, the J-transfer time conveniently also acts as a perfect T_2 filter to filter those signals out and obtain perfect de-crowding of the H8 region. The TOCSY version of the SELOPE idea might be interesting for RNAs, which are bigger or residues, which have a shorter T_2 due to mobility, albeit residual NH_2 peaks being possible.

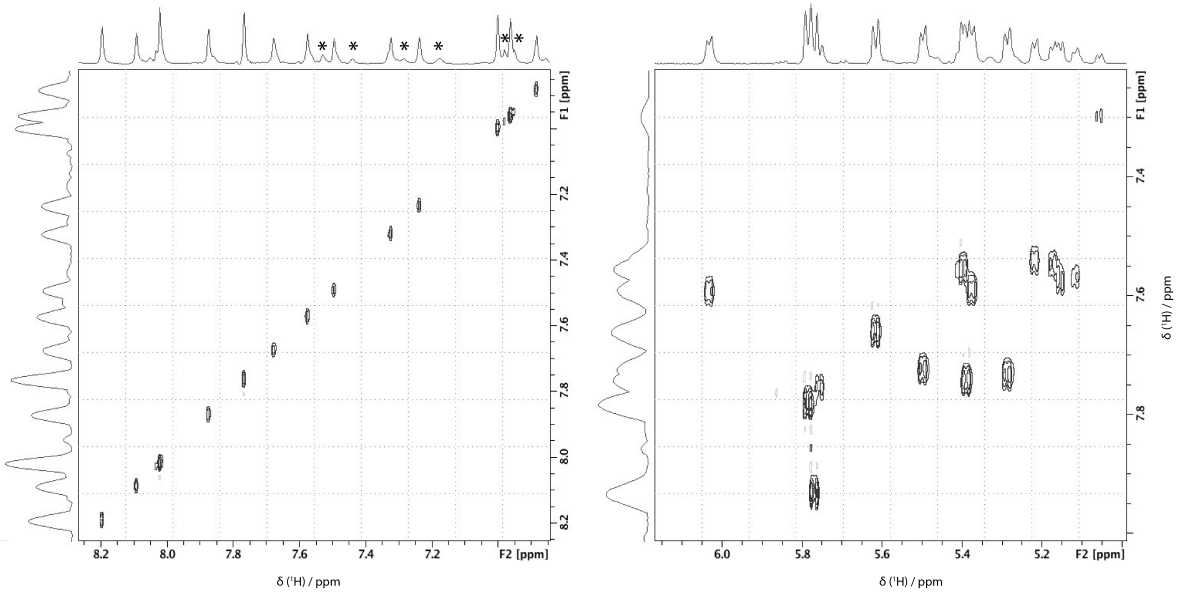

Figure S39. H8 and H6-H5 region of the acquired 2D H8/H6-H5 spectrum of GUC with a 50ms TOCSY transfer to fully transfer H5 magnetization to H6. For this spectrum 44 FIDs were recorded for an indirect dimension of 1.8 ppm spectral width. 16 scans were recorded per increment with a recovery delay of 1.5 s leading to an overall experimental time of 26 min. Asterisks indicate residual NH_2 signals.

This TOCSY can then also be combined with other pulse sequence elements such as spin locks to obtain resolution when measuring ^{1}H $R_{1\rho}$. In this case, the TOCSY transfer adds a 50 ms spin lock to the spin lock needed for the $R_{1\rho}$ measurement. The duration of a SL that can be applied to a sample is hardware limited and longer durations cause heating of the sample. In our case we did not experience any problems of peaks relaxing during the SELOPE transfer, we therefore decided against using the TOCSY transfer. This enabled us to use all the available SL duration for the $R_{1\rho}$ spin lock. After all, long SL times allow measuring faster exchange contributions – one of the advantages of using protons as probes for conformational exchange.

6. REFERENCES

[1] H. Geen, R. Freeman, *Journal of Magnetic Resonance (1969)* **1991**, *93*, 93–141.
[2] T. L. Hwang, A. J. Shaka, *Journal of Magnetic Resonance, Series A* **1995**, *112*, 275–279.
[3] M. Piotto, V. Saudek, V. Sklenář, *Journal of Biomolecular NMR* **1992**, *2*, 661–665.
[4] D. Marion, M. Ikura, R. Tschudin, A. Bax, *Journal of Magnetic Resonance (1969)* **1989**, *85*, 393–399.
[5] C. Altona, M. Sundaralingam, *Journal of the American Chemical ...* **1973**.
[6] S.-H. Bae, H.-K. Cheong, J.-H. Lee, C. Cheong, M. Kainosho, B.-S. Choi, *PNAS* **2001**, *98*, 10602–10607.
[7] S. Flodell, J. Schleucher, J. Cromsigt, H. Ippel, K. Kidd-Ljunggren, S. Wijmenga, *Nucleic Acids Research* **2002**, *30*, 4803–4811.
[8] E. Steiner, J. Schlagnitweit, P. Lundström, K. Petzold, *Angew. Chem. Int. Ed. Engl.* **2016**, *55*, 15869–15872.
[9] A. G. Palmer, F. Massi, *Chem. Rev.* **2006**, *106*, 1700–1719.
[10] S. R. Hartmann, E. L. Hahn, *Physical Review* **1962**, *128*, 2042–2053.
[11] SpinDynamica code for Mathematica, programmed by Malcolm H. Levitt, with Contributions from Iyrki Rantaharju, Andreas Brinkmann and Soumya Singha Roy. Available at www.spindynamica.soton.ac.uk
[12] H. Desvaux, N. Birlirakis, C. Wary, P. Berthault, *Molecular Physics* **1995**, *86*, 1059–1073.
[13] R. K. Gupta, A. G. Redfield, *Science* **1970**, *169*, 1204–1206.
[14] A. N. Lane, T. C. Jenkins, T. Brown, S. Neidle, *Biochemistry* **1991**, *30*, 1372–1385.
[15] P. L. Weber, S. C. Brown, L. Mueller, *Biochemistry* **1987**, *26*, 7282–7290.
[16] A. C. Wang, A. Bax, *Journal of the American Chemical Society* **1996**, *118*, 2483–2494.

7. PULSE PROGRAMS

All pulse programs were written and tested on a Bruker Avance III spectrometer using Topspin 3.2 software.

2D SELOPE

```
;SELOPE_2D.js
;2D 1H-1H correlation experiment using selective excitation and J-tranfer
;J. Schlagnitweit, E. Steiner, H. Karlsson, K. Petzold
;2017


prosol relations=<triple>


#include <Avance.incl>
#include <Grad.incl>
#include <Delay.incl>


"p2=p1*2"
"d12=20u"


"TAU=de+p1*2/3.1416+50u"

;"spoff4=bf1*(cnst21/1000000)-o1"
"spoff4=0"

"acqt0=0"
baseopt_echo


"d0=3u"
"in0=inf1"

"d2=d1/2"

"cnst28=0"

1 ze
2 30m

  d1 fq=cnst28:f1
  50u UNBLKGRAD

;  1u
;  p16:gp5
;  d16

;  1u pl0:f1
;  (p13:sp4 ph23):f1
;  1u pl1:f1
;  p1 ph10

;  1u
;  p16:gp3
;  d16   pl0:f1

  (p13:sp4 ph9):f1

  d0

  d5 pl1:f1                 ;INEPT
  p2 ph0
  d5
  p1 ph12

  d5
  p2 ph0
  d5
```

```
  1u fq=cnst29(bf ppm):f1
  50u ;UNBLKGRAD
  p16:gp1
  d16 pl0:f1
  (p12:sp1 ph2:r):f1
  4u
  d12 pl1:f1

  p2 ph3

  4u
  p16:gp1
  d16
  TAU
  p16:gp2
  d16 pl0:f1
  (p12:sp1 ph4:r):f1
  4u
  d12 pl1:f1

  p2 ph5

  4u
  p16:gp2
  d16

  go=2 ph31
  ;30m mc #0 to 2 F1PH(calph(ph23, +90) & calph(ph10, +90) &calph(ph11, +90) &calph(ph21,
+90) &calph(ph22, +90) &calph(ph9, +90), caldel(d0, +in0))
  30m mc #0 to 2 F1PH(calph(ph9, +90), caldel(d0, +in0))
  4u BLKGRAD
exit

ph0=0
ph1=0 0 0 0 2 2 2 2
;ph23=0 0 0 0 0 0 0 0 2 2 2 2 2 2 2 2
ph2=0 1
ph3=2 3
ph4=0 0 1 1
ph5=2 2 3 3
ph9= 0 0 0 0 2 2 2 2
ph12=3
ph31=0 2 2 0 2 0 0 2 ;2 0 0 2 0 2 2 0



;pl0 : 0W
;pl1 : f1 channel - power level for pulse (default)
;sp1 : f1 channel - shaped pulse 180 degree
;sp4 : f1 channel - 90 sel pulse power level
;p1 : f1 channel -  90 degree high power pulse
;p2 : f1 channel - 180 degree high power pulse
;p12: f1 channel - 180 degree shaped pulse (Squa100.1000)   [2 msec]
;p13: f1 channel -  90 selective pulse (e.g. H8/H6 region) (Eburp2.1000)
;p16: homospoil/gradient pulse
;d1 : relaxation delay; 1-5 * T1
;d12: delay for power switching                              [20 usec]
;d16: delay for homospoil/gradient recovery
;d5: INEPT delay ~25ms, use 1/4J
;ns: 8 * n, total number of scans: NS * TD0
;ds: 4
;cnst29: chem. shift [ppm] of water signal

;for z-only gradients:
;gpz1: 31%
;gpz2: 11%
;gpz3: 49%

;use gradient files:
;gpnamX: SMSQ10.100
```

2D $R_{1\rho}$ SELOPE

```
;1HR1r_SELOPE_2D.js
;Selective excitation followed by SL and 2D H-H correlation experiment using selective
excitation and J-tranfer
;on-resonance 1HR1rho RD, 2D version
;J. Schlagnitweit, E. Steiner, H. Karlsson, K. Petzold
;2017


prosol relations=<triple>


#include <Avance.incl>
#include <Grad.incl>
#include <Delay.incl>


"p2=p1*2"
"d12=20u"


"TAU=de+p1*2/3.1416+50u"

;"spoff4=bf1*(cnst21/1000000)-o1"
"spoff4=0"

"acqt0=0"
baseopt_echo

"p33=d31"
"p29=d30-p33"
"d29=p29"
"p30=d30"

"d0=3u"
"in0=inf1"

"d2=d1/2"


1 ze
2 30m
  d12 pl0:f1 BLKGRAD

  d12 fq=100000:f1
  d12 pl24:f1
  d12

  if "d29 > 0.0"        ;first heat compensation
       {
       p29 ph0
       2u
       }
   else
       {
       d12
       }
;  d1
;  p1 ph1

  d2 pl25:f1
  p30 ph0           ;secon heat compensation

  d2 fq=cnst28:f1
  50u UNBLKGRAD

  1u
  p16:gp5
  d16

  1u pl0:f1
  (p13:sp4 ph1):f1
  1u pl1:f1
  p1 ph10
```

```
  1u
  p16:gp3
  d16    pl0:f1

  ;p1 ph11

       (p13:sp4 ph11):f1
       ;(p11:sp6 ph11):f1              ;adiabatic ramp
                  1u
       1u pl24:f1
       (p33 ph21):f1            ;spin-lock
       1u
       1u pl0:f1
       (p11:sp5 ph21):f1        ;adiabatic ramp

  1u
  p16:gp4
  d16
  (p13:sp4 ph9):f1

  d0

  d5 pl1:f1                 ;INEPT
  p2 ph0
  d5
  p1 ph12

  d5
  p2 ph0
  d5

  1u fq=cnst29(bf ppm):f1
  50u ;UNBLKGRAD
  p16:gp1
  d16 pl0:f1
  (p12:sp1 ph2:r):f1
  4u
  d12 pl1:f1

  p2 ph3

  4u
  p16:gp1
  d16
  TAU
  p16:gp2
  d16 pl0:f1
  (p12:sp1 ph4:r):f1
  4u
  d12 pl1:f1

  p2 ph5

  4u
  p16:gp2
  d16

  go=2 ph31
  30m mc #0 to 2 F1PH(calph(ph1, +90) & calph(ph10, +90) &calph(ph11, +90) &calph(ph21,
+90) &calph(ph9, +90), caldel(d0, +in0))
  4u BLKGRAD
exit

ph0=0
ph1=0 0 0 0 2 2 2 2
ph2=0 1
ph3=2 3
ph4=0 0 1 1
ph5=2 2 3 3
ph9= 0 0 0 0 0 0 0 0 2 2 2 2 2 2 2 2
ph10=2 2 2 2 0 0 0 0
ph11=0 0 0 0 2 2 2 2
ph21=1 1 1 1 3 3 3 3
ph12=3
ph31=0 2 2 0 0 2 2 0 2 0 0 2 2 0 0 2
```

```
;pl0 : 0W
;pl1 : f1 channel - power level for pulse (default)
;pl24: SL power level
;pl25: extra heat comp power level
;sp1 : f1 channel - shaped pulse 180 degree
;sp4 : f1 channel - 90 sel pulse power level
;sp5 : adiabatic ramp (=pl24)
;p1 : f1 channel -  90 degree high power pulse
;p2 : f1 channel - 180 degree high power pulse
;p12: f1 channel - 180 degree shaped pulse Water Sup (Squa100.1000)   [2 msec]
;p11: f1 channel - adiabatic ramp for spin-lock (tanhtan) [4ms]
;p13: f1 channel -  90 selective pulse (e.g. H8/H6 region) (Eburp2.1000)
;p16: homospoil/gradient pulse
;d1 : relaxation delay; 1-5 * T1
;d12: delay for power switching                              [20 usec]
;d16: delay for homospoil/gradient recovery
;d30: maximum relaxation delay to be used in the whole set of exps
;d31: relaxation delay during SL
;d5: INEPT delay use 1/4J
;ns: 16 * n, total number of scans: NS * TD0
;ds: 16
;cnst29: chem. shift [ppm] of water signal


;for z-only gradients:
;gpz1: 31%
;gpz2: 11%
;gpz3: 49%
;gpz4: 17%
;gpz5: 27%

;use gradient files:
;gpnamX: SMSQ10.100
```

1D $R_{1\rho}$ SELOPE (pseudo 2D, for on-resonance RD)

```
;1HR1r_SELOPE_onres1D.js
;Selective excitation followed by SL and 2D H-H correlation experiment using selective
excitation and J-tranfer
;on-resonance 1HR1rho RD, 1D version
;set up as pseudo-2D with vd-list for variable SL length
;J. Schlagnitweit, E. Steiner, H. Karlsson, K. Petzold
;2017


prosol relations=<triple>


#include <Avance.incl>
#include <Grad.incl>
#include <Delay.incl>


"p2=p1*2"
"d12=20u"


"TAU=de+p1*2/3.1416+50u"

;"spoff4=bf1*(cnst21/1000000)-o1"
"spoff4=0"

"acqt0=0"
baseopt_echo

"p33=d31"
"p29=d30-p33"
"d29=p29"
"p30=d30"

"d0=3u"
"in0=inf1"
```

```
"d2=d1/2"

"cnst28=0"


1 ze
2 30m
  d12 pl0:f1 BLKGRAD

  "p33=vd"
  "p29=d30-p33"
  "d29=d30-p33"
  "p30=d30"

  d12 fq=100000:f1
  d12 pl24:f1
  d12

  if "d29 > 0.0"        ;heat compensation block 1
       {
       p29 ph0
       2u
       }
   else
       {
       d12
       }
;  d1
;  p1 ph1

  d2 pl25:f1        ;heat compensation block 2
  p30 ph0

  d2 fq=cnst28:f1
  50u UNBLKGRAD

  1u
  p16:gp5
  d16

  1u pl0:f1
  (p13:sp4 ph23):f1
  1u pl1:f1
  p1 ph10

  1u
  p16:gp3
  d16    pl0:f1

  ;p1 ph11

       (p13:sp4 ph11):f1
                  1u
       1u pl24:f1
       (p33 ph21):f1            ;spin-lock
       1u
       1u pl1:f1
       (p1 ph22):f1

  1u
  p16:gp4
  d16    pl0:f1
  (p13:sp4 ph9):f1

  d0

  d5 pl1:f1                 ;INEPT
  p2 ph0
  d5
  p1 ph12

  d5
  p2 ph0
  d5

  1u fq=cnst29(bf ppm):f1   ;excitation sculpting, water suppression
```

```
  50u ;UNBLKGRAD
  p16:gp1
  d16 pl0:f1
  (p12:sp1 ph2:r):f1
  4u
  d12 pl1:f1

  p2 ph3

  4u
  p16:gp1
  d16
  TAU
  p16:gp2
  d16 pl0:f1
  (p12:sp1 ph4:r):f1
  4u
  d12 pl1:f1

  p2 ph5

  4u
  p16:gp2
  d16

  go=2 ph31
  30m wr #0 if #0 ivd
  lo to 1 times td1
  ;30m mc #0 to 2 F1PH(calph(ph23, +90) & calph(ph10, +90) &calph(ph11, +90) &calph(ph21,
+90) &calph(ph22, +90) &calph(ph9, +90), caldel(d0, +in0))
  4u BLKGRAD
exit

ph0=0
ph1=0 0 0 0 2 2 2 2
ph23=0 0 0 0 0 0 0 0 2 2 2 2 2 2 2 2
ph2=0 1
ph3=2 3
ph4=0 0 1 1
ph5=2 2 3 3
ph9= 0 0 0 0 2 2 2 2
ph10=2 2 2 2 ;0 0 0 0
ph11=0 0 0 0 2 2 2 2
ph21=1 1 1 1 3 3 3 3
ph22=2 2 2 2 0 0 0 0
ph12=3
ph31=0 2 2 0 2 0 0 2 2 0 0 2 0 2 2 0



;pl0 : 0W
;pl1 : f1 channel - power level for pulse (default)
;pl24: SL power level
;pl25: extra heat comp power level
;sp1 : f1 channel - shaped pulse 180 degree
;sp4 : f1 channel - 90 sel pulse power level
;p1 : f1 channel -  90 degree high power pulse
;p2 : f1 channel - 180 degree high power pulse
;p12: f1 channel - 180 degree shaped pulse Water Sup (Squa100.1000)   [2 msec]
;p13: f1 channel -  90 selective pulse (e.g. H8/H6 region) (Eburp2.1000)
;p16: homospoil/gradient pulse
;d1 : relaxation delay; 1-5 * T1
;d12: delay for power switching                                [20 usec]
;d16: delay for homospoil/gradient recovery
;d30: maximum relaxation delay to be used in the whole set of exps
;d31: relaxation delay during SL
;d5: INEPT delay ~25ms, use 1/4J
;ns: 16 * n
;ds: 16
;cnst29: chem. shift [ppm] of water signal

;for z-only gradients:
;gpz1: 31%
;gpz2: 11%
;gpz3: 49%
;gpz4: 17%
;gpz5: 27%
```

```
;use gradient files:
;gpnamX: SMSQ10.100
```

1D $R_{1\rho}$ SELOPE (pseudo 2D, for off-resonance RD)

```
;1HR1r_SELOPE_offres1D.js
;Selective excitation followed by SL and 2D H-H correlation experiment using selective
excitation and J-tranfer
;off-resonance 1HR1rho RD, 1D version
;set up as pseudo-2D with vd-list for variable SL length
;J. Schlagnitweit, E. Steiner, H. Karlsson, K. Petzold
;2017
;
;$CLASS=HighRes
;$DIM=1D
;$TYPE=
;$SUBTYPE=
;$COMMENT=


prosol relations=<triple>


#include <Avance.incl>
#include <Grad.incl>
#include <Delay.incl>


"p2=p1*2"
"d12=20u"

"cnst21=o1/sfo1"
"cnst12=(sqrt(plw24/plw1))*(2.5/p1)*100000"

"TAU=de+p1*2/3.1416+50u"

"spoff4=0"
;"spoff4=bf1*(cnst21/1000000)-o1"

"acqt0=0"
baseopt_echo

"p33=d31"
"p29=d30-p33"
"d29=p29"
"p30=d30"

"d0=3u"
"in0=inf1"

"d2=d1/2"

"p19=p1*atan(cnst12/abs(cnst30))*2/3.14159"
"cnst31=cnst21+(cnst30/sfo1)"

1 ze
2 30m
  d12 pl0:f1 BLKGRAD

  "p33=vd"
  "p29=d30-p33"
  "d29=d30-p33"
  "p30=d30"

  d12 fq=100000:f1
  d12 pl24:f1
  d12

  if "d29 > 0.0"        ;heat compensation block
       {
       p29 ph0
       2u
       }
```

```
   else
       {
       d12
       }
;  d1
;  p1 ph1

  d2 pl25:f1
  p30 ph0

  d2 fq=cnst28:f1
  50u UNBLKGRAD

  1u
  p16:gp5
  d16

  1u pl0:f1
  (p13:sp4 ph23):f1
  1u pl1:f1
  p1 ph10

  1u
  p16:gp3
  d16    pl1:f1

  ;p1 ph11

 if "cnst30>0"
       {
       p19 ph21
       1u
       2u fq=cnst31(bf ppm):f1
       1u pl24:f1
       (p33 ph11):f1            ;spin-lock
       1u
       2u fq=cnst28:f1
       1u pl1:f1
       p19 ph22
       }
else
       {
       p19 ph22
       1u
       2u fq=cnst31(bf ppm):f1
       1u pl24:f1
       (p33 ph11):f1            ;spin-lock
       1u
       2u fq=cnst28:f1
       1u pl1:f1
       p19 ph21
       }

  1u
  p16:gp4
  d16
  (p13:sp4 ph9):f1

  d0

  d5 pl1:f1                ;INEPT
  p2 ph0
  d5
  p1 ph12

  d5
  p2 ph0
  d5

  1u fq=cnst29(bf ppm):f1
  50u ;UNBLKGRAD
  p16:gp1
  d16 pl0:f1
  (p12:sp1 ph2:r):f1
  4u
  d12 pl1:f1
```

```
  p2 ph3

  4u
  p16:gp1
  d16
  TAU
  p16:gp2
  d16 pl0:f1
  (p12:sp1 ph4:r):f1
  4u
  d12 pl1:f1

  p2 ph5

  4u
  p16:gp2
  d16

  go=2 ph31
  30m wr #0 if #0 ivd
  lo to 1 times td1
  ;30m mc #0 to 2 F1PH(calph(ph1, +90) & calph(ph10, +90) &calph(ph11, +90) &calph(ph21,
+90) &calph(ph9, +90), caldel(d0, +in0))
  4u BLKGRAD
exit

ph0=0
ph1=0 0 0 0 2 2 2 2
ph23=0 0 0 0 0 0 0 0 2 2 2 2 2 2 2 2
ph2=0 1
ph3=2 3
ph4=0 0 1 1
ph5=2 2 3 3
ph9= 0 0 0 0 2 2 2 2
ph10=2 2 2 2 ;0 0 0 0
ph11=0 0 0 0 2 2 2 2
ph21=1 1 1 1 3 3 3 3
ph22=3 3 3 3 1 1 1 1
ph12=3
ph31=0 2 2 0 2 0 0 2 2 0 0 2 0 2 2 0


;pl0 : 0W
;pl1 : f1 channel - power level for pulse (default)
;pl24: SL power level
;pl25: extra heat comp power level
;sp1 : f1 channel - shaped pulse 180 degree
;sp4 : f1 channel - 90 sel pulse power level
;p1 : f1 channel -  90 degree high power pulse
;p2 : f1 channel - 180 degree high power pulse
;p12: f1 channel - 180 degree shaped pulse Water Sup (Squa100.1000)   [2 msec]
;p13: f1 channel -  90 selective pulse (e.g. H8/H6 region) (Eburp2.1000)
;p16: homospoil/gradient pulse
;d1 : relaxation delay; 1-5 * T1
;d12: delay for power switching                                [20 usec]
;d16: delay for homospoil/gradient recovery
;d30: maximum relaxation delay to be used in the whole set of exps
;d31: relaxation delay during SL
;d5: INEPT delay ~25ms, use 1/4J
;ns: 16 * n
;ds: 4
;cnst29: chem. shift [ppm] of water signal
;cnst12: sl strength
;cnst30: sl offset
;cnst21: o1p

;for z-only gradients:
;gpz1: 31%
;gpz2: 11%
;gpz3: 49%
;gpz4: 17%
;gpz5: 27%

;use gradient files:
;gpnamX: SMSQ10.100
```

CEST SELOPE

```
;1HCEST_SELOPE.js
;Selective excitation followed by SL and 2D H-H correlation experiment using selective
excitation and J-tranfer
;on-resonance 1HR1rho RD, 2D version
;J. Schlagnitweit, E. Steiner, H. Karlsson, K. Petzold
;2017


prosol relations=<triple>


#include <Avance.incl>
#include <Grad.incl>
#include <Delay.incl>


"p2=p1*2"
"d12=20u"


"TAU=de+p1*2/3.1416+50u"

;"spoff4=bf1*(cnst21/1000000)-o1"
"spoff4=0"

"acqt0=0"
baseopt_echo

"p33=d31"
"p29=d30-p33"
"d29=p29"
"p30=d30"

"d0=3u"
"in0=inf1"

"d2=d1/2"


1 ze
2 30m
  d12 pl0:f1 BLKGRAD

  d12 fq=100000:f1
  d12 pl24:f1
  d12

  if "d29 > 0.0"        ;first heat compensation
       {
       p29 ph0
       2u
       }
   else
       {
       d12
       }
;  d1
;  p1 ph1

  d2 pl25:f1
  p30 ph0           ;second heat compensation

  d2 fq=cnst28:f1
  50u UNBLKGRAD

  1u
  p16:gp5
  d16

  1u pl0:f1
  (p13:sp4 ph1):f1
  1u pl1:f1
  p1 ph10
```

```
  1u
  p16:gp3
  d16    pl0:f1

       1u
       2u fq=cnst31:f1

if "p33 > 0.0"
       {
       1u pl24:f1
       (p33 ph11):f1            ;spin-lock
       1u
       }
       2u fq=cnst28:f1

  1u
  p16:gp4
  d16
  (p13:sp4 ph9):f1

  d0

  d5 pl1:f1                 ;INEPT
  p2 ph0
  d5
  p1 ph12

  d5
  p2 ph0
  d5

  1u fq=cnst29(bf ppm):f1
  50u ;UNBLKGRAD
  p16:gp1
  d16 pl0:f1
  (p12:sp1 ph2:r):f1
  4u
  d12 pl1:f1

  p2 ph3

  4u
  p16:gp1
  d16
  TAU
  p16:gp2
  d16 pl0:f1
  (p12:sp1 ph4:r):f1
  4u
  d12 pl1:f1

  p2 ph5

  4u
  p16:gp2
  d16

  go=2 ph31
  30m mc #0 to 2 F1PH(calph(ph1, +90) & calph(ph10, +90) &calph(ph11, +90) &calph(ph21,
+90) &calph(ph9, +90), caldel(d0, +in0))
  4u BLKGRAD
exit

ph0=0
ph1=0 0 0 0 2 2 2 2
ph2=0 1
ph3=2 3
ph4=0 0 1 1
ph5=2 2 3 3
ph9= 0 0 0 0 0 0 0 0 2 2 2 2 2 2 2 2
ph10=2 2 2 2 ;0 0 0 0
ph11=0 0 0 0 ;2 2 2 2
ph21=1 1 1 1 3 3 3 3
ph12=3
ph31=0 2 2 0 0 2 2 0 2 0 0 2 2 0 0 2
```

```
;pl0 : 0W
;pl1 : f1 channel - power level for pulse (default)
;pl24: SL power level
;pl25: extra heat comp power level
;sp1 : f1 channel - shaped pulse 180 degree
;sp4 : f1 channel - 90 sel pulse power level
;p1 : f1 channel -  90 degree high power pulse
;p2 : f1 channel - 180 degree high power pulse
;p12: f1 channel - 180 degree shaped pulse Water Sup (Squa100.1000)   [2 msec]
;p13: f1 channel -  90 selective pulse (e.g. H8/H6 region) (Eburp2.1000)
;p16: homospoil/gradient pulse
;d1 : relaxation delay; 1-5 * T1
;d12: delay for power switching                              [20 usec]
;d16: delay for homospoil/gradient recovery
;d30: maximum relaxation delay to be used in the whole set of exps
;d31: relaxation delay during SL
;d5: INEPT delay use 1/4J
;ns: 16 * n, total number of scans: NS * TD0
;ds: 16
;cnst29: chem. shift [ppm] of water signal
;cnst31: SL offset


;for z-only gradients:
;gpz1: 31%
;gpz2: 11%
;gpz3: 49%
;gpz4: 17%
;gpz5: 27%

;use gradient files:
;gpnamX: SMSQ10.100
```